

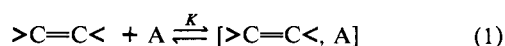
Azoalkanes as Electron Donors in Charge-Transfer Complexes. Molecular Structures with Sacrificial (π^* , σ^*) and Incevalent (ν) Electron Acceptors

S. C. Blackstock and J. K. Kochi*

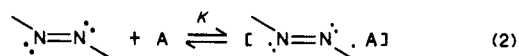
Contribution from the Department of Chemistry, University of Houston, University Park, Houston, Texas 77004. Received September 17, 1986

Abstract: A novel series of electron donor–acceptor (EDA) complexes of various azoalkanes with the three unique types of electron acceptors are characterized in solution from their charge-transfer (CT) spectra. Among azoalkanes, the electron-rich diazabicyclooctene (DBO) and -heptene (DBH) afford isolable complexes with the prototypical acceptors tetracyanoethylene (π^*), carbon tetrabromide (σ^*), and silver(I) nitrate (ν), but the electron-deficient azobisisobutyronitrile (AIBN) does not. Quantitative evaluation of the formation constants K by the Benesi–Hildebrand method indicates that these azoalkane complexes are moderately weak in solution. However, the insolubility of the electron donor–acceptor complexes from DBO/TCNE, DBO/ CBr_4 , and DBO/ AgNO_3 pairs in ethereal solutions allows single crystals to be carefully grown. X-ray crystallography establishes the existence of three unique types of molecular structures for these azo complexes. Thus the 1:1 complex with AgNO_3 in Figure 13 consists of a dimeric six-membered ring in which each silver(I) serves as a bridge between azo groups via the nitrogen lone pairs (n). On the other hand, the 1:1 complex with CBr_4 in Figure 9 consists of an infinite chain with alternating azo units n -bound by a pair of bromine bridges—reminiscent of that previously established for difunctional amines such as in the dabco- CBr_4 complex. The unusual 2:1 complex with TCNE in Figure 8 consists of a sandwich structure in which the central $\text{C}=\text{C}$ unit is equally bound on each planar face by both nitrogen atoms of the azo moiety. The HOMO–LUMO interactions in these donor–acceptor complexes are considered in the context of the anti-bonding (n_-) and bonding (n_+) combination of the azo n -orbitals. The charge-transfer photochemistry of various EDA complexes of azoalkanes is examined briefly. The photochemical efficiency is qualitatively discussed in terms of the stability of the azoalkane cation–radical in the CT excited state, as independently evaluated by ESR studies following their formation by the freon matrix (Cl_3CF) method.

Azoalkanes are isoelectronic with alkenes. Although both classes of unsaturated compounds are electron rich, only alkenes are known to interact readily with various types of electrophiles and electron acceptors (A) to form molecular complexes reversibly,^{1,2} i.e.

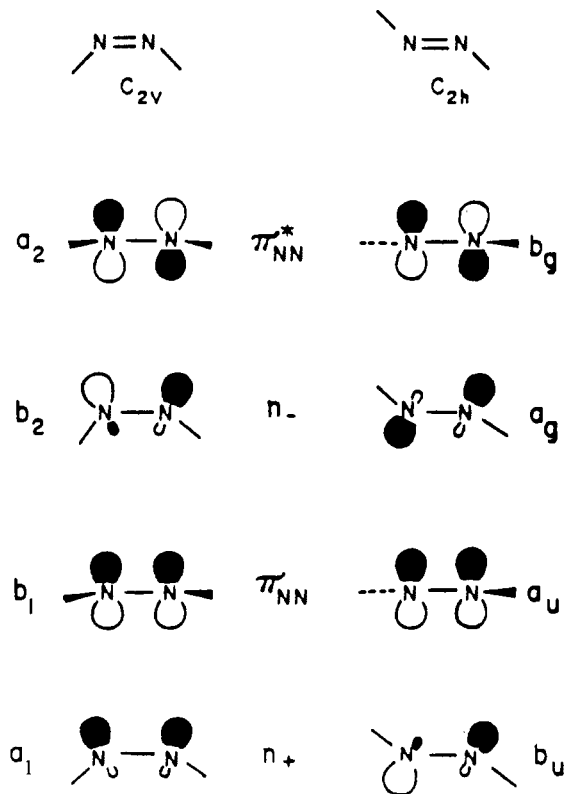


When the electron acceptor is a halogen such as Br_2 or Cl_2 ³ or mercury(II),⁴ tetranitromethane,⁵ etc., the electron donor–acceptor (EDA) complex in eq 1 is the reactive intermediate leading to the electrophilic addition reactions.⁶ In these alkene complexes, the charge-transfer (CT) interaction largely derives from the π -HOMO of the carbon–carbon double bond and the LUMO of the electron acceptor.⁷ On the other hand, if azoalkanes are considered as electron donors in a similar capacity, i.e.



there are *two* sites which are potentially available for this CT interaction—namely, the azo linkage (π) as well as the lone-pair (n) on each nitrogen center. Electronically, the latter are split into an in-phase or bonding combination (n_+) and an out-of-phase

Chart I. Designation of the n and π Orbitals in Cis and Trans Azo Chromophores According to Descending Energy (Top to Bottom)⁹



or antibonding combination (n_-), as illustrated in Chart I.⁸ The magnitude of the splitting (Δn) differs somewhat in cis (C_{2v}) and trans (C_{2h}) chromophores, and it also depends on N-alkyl sub-

(1) Foster, R. *Organic Charge-Transfer Complexes*; Academic: New York, 1969.

(2) (a) Andrews, L. J.; Keefer, R. M. *Molecular Complexes in Organic Chemistry*; Holden-Day: San Francisco, 1964. See, also: (b) Briegleb, *Electronen Donator-Acceptor Komplexe*; Springer Verlag: Berlin, 1961.

(3) (a) Buckles, R. E.; Yuk, J. P. *J. Am. Chem. Soc.* **1953**, *75*, 5048. (b) Dubois, J. E.; Garnier, F. *Spectrochim. Acta Part A* **1967**, *23A*, 2279; *Tetrahedron Lett.* **1965**, 3961.

(4) Eliezer, I.; Avinur, P. *J. Chem. Soc., Faraday Trans. 2* **1974**, *70*, 1316. Damude, L. C.; Dean, P. A. W. *J. Chem. Soc., Chem. Commun.* **1978**, 1083.

(5) Altukhov, R. V.; Perekalin, V. V. *Russ. Chem. Rev.* **1976**, *45*, 1052.

(6) Fukuzumi, S.; Kochi, J. K. *J. Am. Chem. Soc.* **1981**, *103*, 2783; *Int. J. Chem. Kinetics* **1983**, *15*, 249; *J. Am. Chem. Soc.* **1982**, *104*, 7599. See, also: Fukuzumi, S.; Kochi, J. K. *J. Am. Chem. Soc.* **1981**, *103*, 7240; *Tetrahedron* **1982**, *38*, 1035.

(7) Person, W. B.; Mulliken, R. S. *Molecular Complexes, A Lecture and Reprint Volume*; Wiley: New York, 1969.

(8) Haselbach, E.; Heilbronner, E. *Helv. Chim. Acta* **1970**, *53*, 684. Haselbach, E.; Schmelzer, S. *Helv. Chim. Acta* **1971**, *54*, 1575.

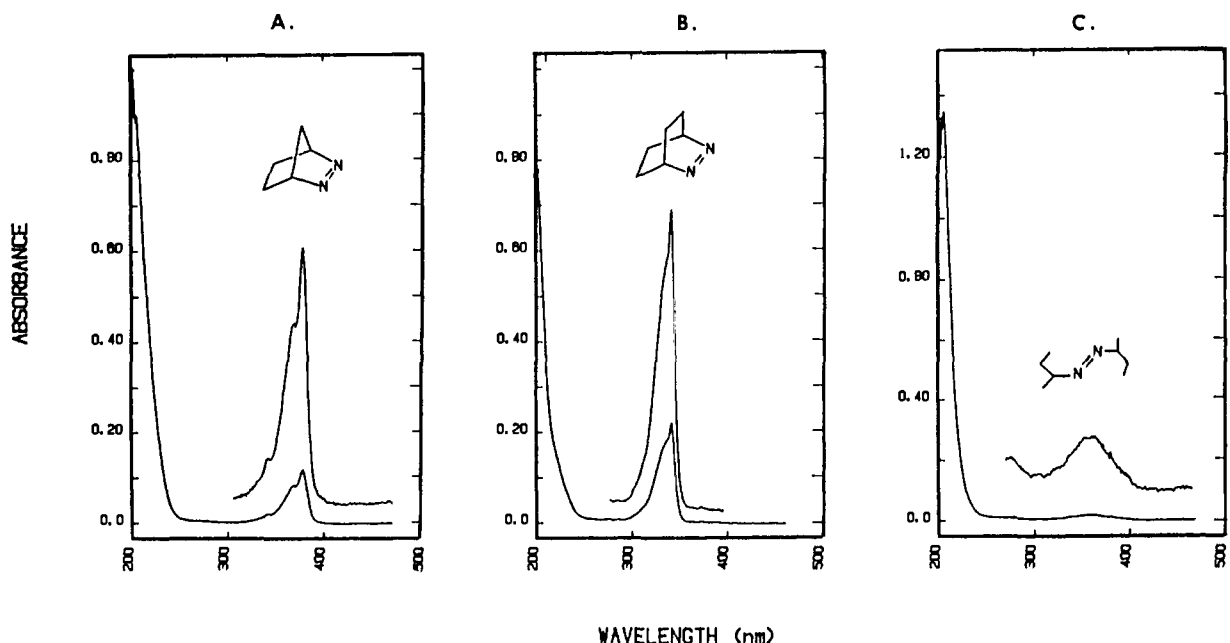


Figure 1. The absorption spectrum of 10^{-3} M solutions of (A) DBH, (B) DBO, and (C) AB in acetonitrile. The insets show the absorbances of the n, π^* bands at $\times 5$, $\times 3$, and $\times 10$ enhancement.

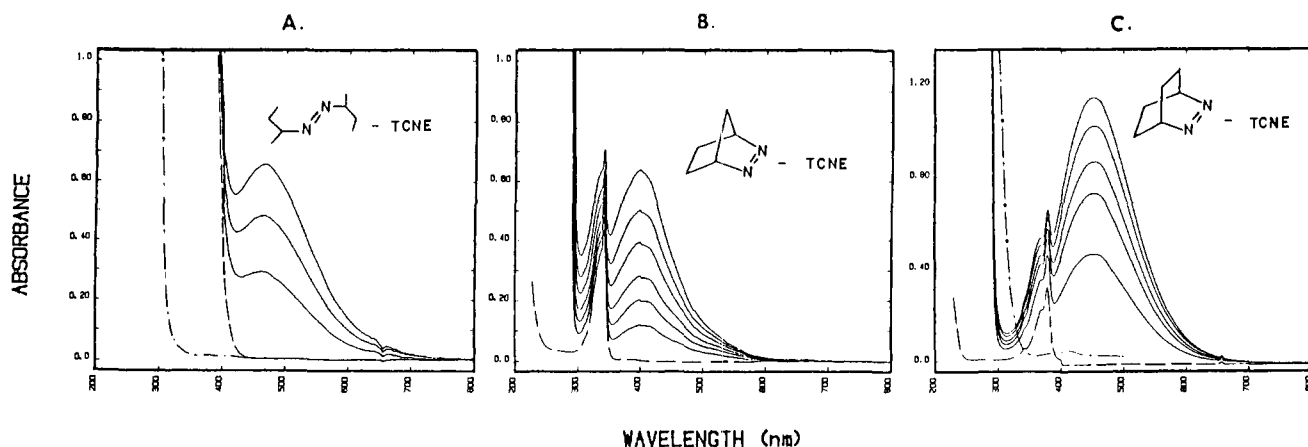


Figure 2. Charge-transfer bands of the EDA complexes of (A) 0.14 M AB, (B) 2.6×10^{-3} M DBH, and (C) 3.0×10^{-3} M DBO with various concentrations of TCNE (see Experimental Section). For comparison, the absorption spectra of the uncomplexed azoalkanes are indicated by (---) and TCNE alone by (-.-) in acetonitrile solution.

stitution and the C—N=N or "bite" angle.^{9,10} The orbital energies in azoalkanes generally decrease in the order n , π , n , in both *cis*- and *trans*-azoalkanes.¹¹

Despite the strong structural and electronic similarity of azoalkanes with alkenes, an examination of the extant literature does not reveal similar examples of molecular complex formation, especially those from which CT transitions are observed. For example, charge-transfer absorption bands are commonly observed immediately upon mixing alkenes with a variety of electron acceptors such as tetracyanoethylene (TCNE), bromine, mercury(II) salts, etc.^{1,6,12} By way of contrast, there are no reports of analogous CT absorptions associated with any combination of azoalkane and electron acceptor (electrophile).

In order to establish that azoalkanes can be viable electron donors, we initially examined the spectral changes accompanying the interaction of tetracyanoethylene, tetrabromomethane, and silver(I) as the prototypical examples of the three classes of electron acceptors, viz., π^* , σ^* , and v , as originally defined by Mulliken.¹³ In each case, these observations were followed by the spectrophotometric measurement of the formation constant of the EDA complexes in solution and the isolation of single crystals for X-ray crystallographic determination. The latter provided a structural basis for the donor-acceptor interaction from the HOMO of the azoalkane to the different orbital symmetry available in the LUMO's of TCNE, CBr_4 , and Ag(I) .

Results and Discussion

Four types of azo compounds were chosen as representative electron donors which differ in the stereochemistry about the N=N bond and in the magnitude of the vertical ionization potential,^{9,14,15} i.e.

(9) Houk, K. N.; Chang, Y.-M.; Engel, P. S. *J. Am. Chem. Soc.* **1975**, *97*, 1824. We thank Dr. Houk for his kind permission to reproduce Figure 1.

(10) (a) Baird, N. C.; Demago, P.; Swenson, J. R.; Usselman, M. C. *J. Chem. Soc., Chem. Commun.* **1973**, 314. (b) Brogli, F.; Eberbach, W.; Haselbach, E.; Heilbronner, E.; Hornung, V.; Lemal, D. M. *Helv. Chim. Acta* **1973**, *56*, 1933. (c) See, also: Gimarc, B. M. *J. Am. Chem. Soc.* **1970**, *92*, 266.

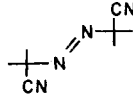
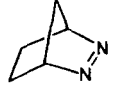
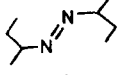
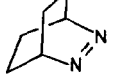
(11) Robin, M. B. In *Chemistry of Hydrazo, Azo and Azoxy Groups*; Patai, S., Ed.; Wiley: New York, 1975.

(12) Melby, L. R. In *Chemistry of the Cyano Group*; Rappoport, Z., Ed.; Wiley: New York, 1970, Chapter 10.

(13) Mulliken, R. S. *J. Phys. Chem., Ithaca*, **1952**, *56*, 801.

(14) Boyd, R. J.; Bünzli, J. C.; Snyder, J. P.; Heyman, M. L. *J. Am. Chem. Soc.* **1973**, *95*, 6478.

(15) The value of IP_v for AB is assumed to be the same as that for *trans*-azoisopropane.⁹

	AIBN (<i>trans</i> -azo-2-cyano-2-propane)	IP _v (eV) 9.62
	DBN (2,3-diazabicyclo[2.2.1]hept-2-ene)	8.96
	AB (<i>trans</i> -azo-2-butane)	8.47
	DBO (2,3-diazabicyclo[2.2.2]octene)	8.32

The absorption spectra of these azo donors in the 300–400-nm region consisted of a weak n, π^* band with the extinction coefficient for the *cis* isomer which is ~ 10 times larger than that for the *trans* isomer,¹⁶ as qualitatively compared in Figure 1.

I. Charge-Transfer Spectra of Azoalkane Complexes with Sacrificial and Inerevalent Electron Acceptors in Solution. When a colorless solution of the azoalkane DBO in either methylene chloride or acetonitrile was mixed with tetracyanoethylene, it immediately turned dark red brown. Pronounced changes in color were also observed when DBO was treated with such common electron acceptors as chloranil (dark yellow), iodine (orange), tetranitromethane (yellow), perfluoroalkyl radical¹⁷ (dark brown), and silver nitrate (yellow). On the other hand, when a colorless solution of the cyano-substituted AIBN in either methylene chloride or acetonitrile was mixed with tetracyanoethylene, no change was observed. Furthermore no new colors were observed when the other electron acceptors chloranil, iodine, tetranitromethane, or perfluoroalkyl radical were treated with AIBN, the colorless solutions remaining unchanged for indefinite periods.

The striking difference in the behavior of DBO and AIBN qualitatively accords with the origin of the colors from the charge-transfer excitation of the azo complex with three electron acceptors.^{1,2} Thus the substantial increase in the ionization potential of the azo donor from 8.3 eV in DBO to 9.6 eV in AIBN is sufficient to cause a very large shift of the yellow-brown colors to beyond the visible region.¹⁹ In order to quantify this conclusion, we monitored the changes in the electronic absorption spectrum of the azo compound (Figure 1) attendant upon the addition of various electron acceptors, as described individually below.

Tetracyanoethylene formed electron donor–acceptor complexes with the azoalkanes AB, DBO, and DBH, as shown in Figure 2 by the appearance of broad absorption bands beyond the low-energy tail of the n, π^* transition of the uncomplexed donors. The positions of the CT bands generally paralleled the trend in the ionization potentials of the azoalkane—the maxima $\lambda_{CT} = 468, 458, \text{ and } 404 \text{ nm}$ for the [AB, TCNE], [DBO, TCNE], and [DBH, TCNE] complexes, respectively, in methylene chloride solution more or less falling in line with the magnitudes of the ionization potentials given above.²⁰ The presence of the intact donors in solution was indicated by the characteristic singlet resonances observed at $\delta 5.03$ and 5.06 for the bridgehead protons of DBO and DBH, respectively, in the ¹H NMR spectra of TCNE solutions of these azoalkanes.^{22,23} When AIBN was treated with

tetracyanoethylene in methylene chloride solutions, no color change was apparent. However, a very weak absorption was discerned with a shoulder at $\sim 410 \text{ nm}$ in the electronic spectrum.

The solvent effect on the CT absorption was relatively minor as indicated by $\lambda_{CT} = 452$ and 400 nm for the DBO–TCNE and DBH–TCNE complexes, respectively, in the more polar acetonitrile solutions.

Carbon tetrabromide interacted immediately with azoalkanes to afford yellow solutions of the EDA complexes. However the examination of the electronic spectra revealed only end absorptions of the CT bands. For example, the absorption spectrum in Figure 3A shows that the color of the DBH–CBr₄ complex was associated with a nondescript red shift in which no distinct CT band was delineated. Visual extrapolation of the prolonged red tail suggested that the CT absorption maximum λ_{CT} was obscured by the azo chromophore and overlapped with the n, π^* transition. The presence of the intact donor was confirmed by the observation of the singlet resonance at $\delta 5.06$ in the ¹H NMR spectrum of the TCNE solution of DBH.

Similarly, the yellow color formed instantly upon the mixing of DBO with carbon tetrabromide was also due to a red shift in the absorption spectrum (Figure 3B), with no resolvable, distinct band apparent. However, it is noteworthy that the displacement of the low-energy tails from 360 to 420 nm in Figure 3 (parts A and B) is similar to the difference in the CT maxima of the corresponding TCNE complexes in Figure 2 (parts A and B). As such, the yellow colors can be reasonably assigned to the charge-transfer excitation of the EDA complexes of carbon tetrabromide with these azoalkanes.

Silver(I) nitrate afforded yellow solutions of the EDA complexes of the azoalkanes DBO and DBH immediately upon mixing the components in acetonitrile, as shown by absorption spectra in Figure 4. The blue shift ($\Delta\lambda_{CT}$) in the CT absorption maxima of the DBO–AgNO₃ complex from $\lambda_{CT} = 470\text{--}414 \text{ nm}$ in the corresponding DBH complex was consistent with the relative donor properties of the uncomplexed azoalkanes, as given by the magnitudes of their ionization potentials (*vide supra*). It is also noteworthy that the magnitude of the energy difference between these CT bands [i.e., $\lambda_{CT}(\text{DBH–Ag}^+) - \lambda_{CT}(\text{DBO–Ag}^+) \equiv 0.36 \text{ V}$] is the same as that observed between the corresponding EDA complexes with TCNE [i.e., $\lambda_{CT}(\text{DBH–TCNE}) - \lambda_{CT}(\text{DBO–TCNE}) \equiv 0.35 \text{ V}$] shown in Figure 2. Such a consistent spectral shift is diagnostic of the charge-transfer origin of these absorption bands according to Mulliken theory.¹⁷ Moreover, the ¹H NMR spectra of the silver(I) solutions containing DBO and DBH indicated that the azoalkane moieties remained intact throughout.^{22,23}

The charge-transfer band of the DBO complex with silver(I) in Figure 4 was insensitive to structural changes in the oxy ligand. For example, the maximum of the CT band for the EDA complex prepared from silver(I) trifluoroacetate occurred at the same position ($\lambda_{CT} = 468 \text{ nm}$ in methylene chloride) as that derived from silver(I) nitrate (*vide supra*). Similarly the CT bands for the complexes derived from silver(I) trifluoromethanesulfonate and silver(I) *p*-toluenesulfonate were essentially the same as those described above.

A close scrutiny of the CT spectrum of the EDA complex from DBO and AgNO₃ in Figure 4A indicated the presence of an intense absorption which lay in the narrow region (360–380 nm) between the CT band and the tail absorptions of the separate donor and acceptor components. Indeed, the serial dilution of the solution of the EDA complex coupled with the spectral subtraction of the uncomplexed DBO and AgNO₃ revealed an additional band with an absorption maximum $\lambda'_{CT} = 389 \text{ nm}$. The same absorption band was more clearly delineated with DBO and AgO₂CCF₃ in methylene chloride,²⁴ and it is illustrated in Figure 5A. A similar treatment of the more strained homologue DBH educed an analogous band centered at $\lambda'_{CT} = 351 \text{ nm}$ (Figure 5B). As such, these high-lying bands must also arise from an electronic transition in the EDA complexes of the azoalkanes with silver(I). Although

(16) Engel, P. S. *Chem. Rev.* **1980**, *80*, 99. See, also: Houk et al. in ref 9.

(17) As perfluoro-2,4-dimethyl-3-ethyl-3-pentyl radical.¹⁸

(18) Scherer, K. V., Jr.; Ono, T.; Yamanouchi, K.; Fernandez, R.; Henderson, P.; Goldwhite, H. *J. Am. Chem. Soc.* **1985**, *107*, 718. For electron acceptor properties, Smart, B. M., private communication.

(19) For weak EDA complexes, $h\nu_{CT} = IP_v - E_a - \omega$ where $h\nu_{CT}$ is the charge-transfer absorption band, E_a the electron affinity of the acceptor, and ω the work term of the ion pair.¹⁷

(20) Note that geometrical differences in EDA complexes of *cis* and *trans* azo complexes are sufficient to alter $h\nu_{CT}$ by causing changes in the work term.

(21) Klingler, R. J.; Fukuzumi, S.; Kochi, J. K. *ACS Symp. Ser.* **1983**, *211*, 117.

(22) Askani, R. *Chem. Ber.* **1965**, *98*, 2551.

(23) Gassman, P. G.; Mansfield, K. T. *Organic Synth.* Wiley: New York, 1973; Collect. Vol. V, p 96.

(24) Silver(I) forms an acetonitrile complex in CH₃CN which shifts the low-energy cutoff to $\sim 360 \text{ nm}$ and partially obscures λ_{CT} .

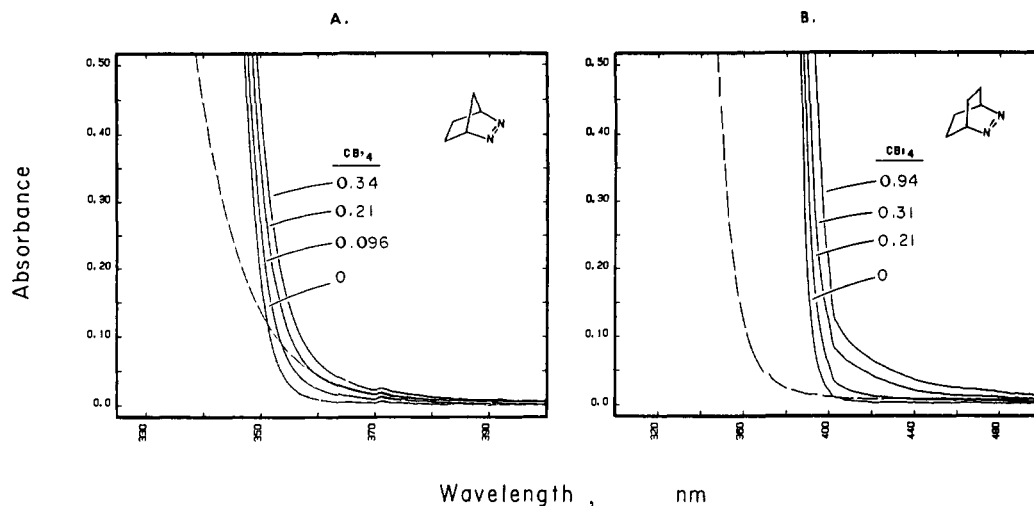


Figure 3. The red shift in the absorption spectrum accompanying the addition on increasing amounts of CBr_4 to (A) 0.012 M DBH and (B) 0.021 M DBO in CH_3CN . For comparison, the absorptions due to (a) 0.34 M and (b) 0.98 M CBr_4 alone are indicated by (---).

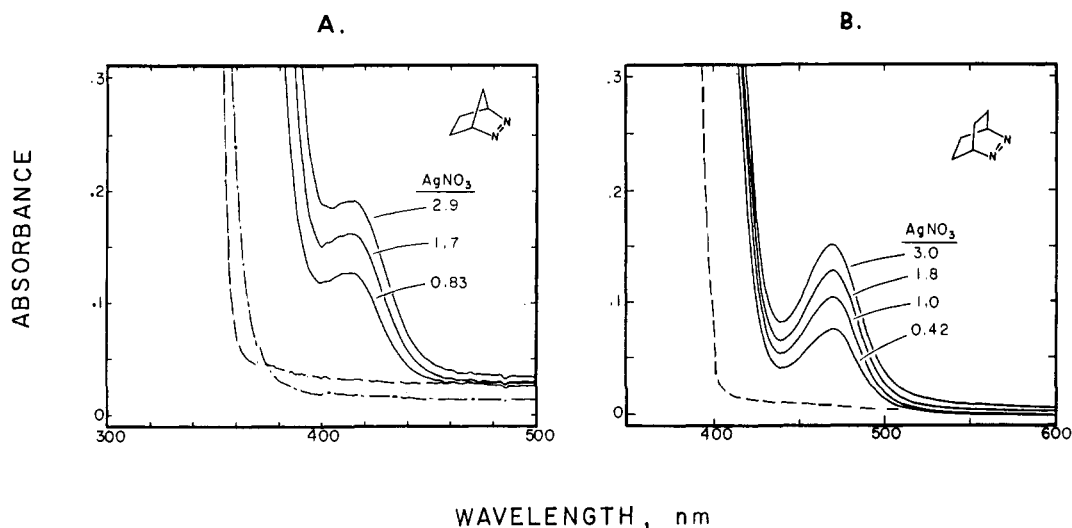


Figure 4. Charge-transfer bands of the EDA complexes from (A) 0.090 M DBH and (B) 0.091 M DBO with various amounts of silver(I) nitrate in acetonitrile, as indicated. For comparison, the absorptions of (A) 0.090 M DBH and (B) 0.091 M DBO alone are indicated by (---) and (A) 2.9 M AgNO_3 alone by (—·—).

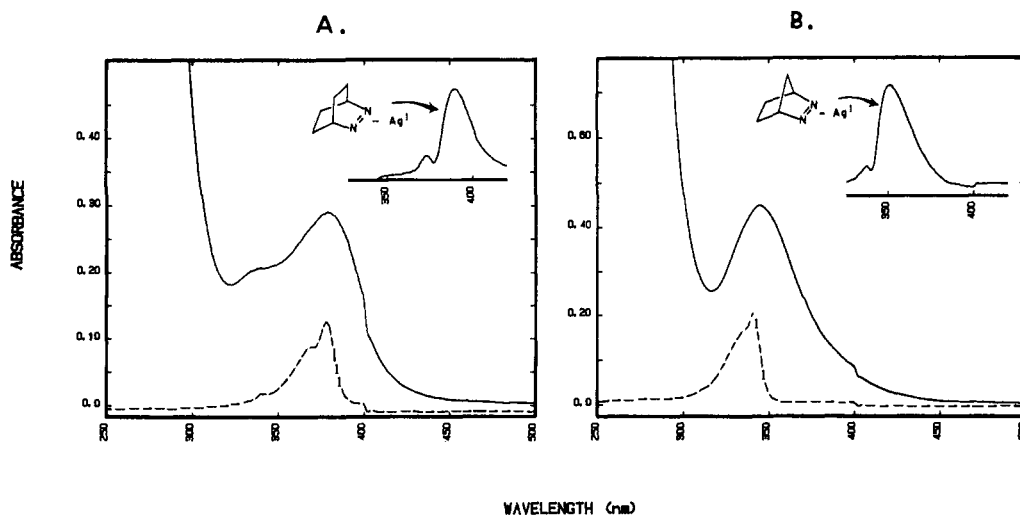


Figure 5. High-lying absorption band (inset) by the spectral subtraction from the charge-transfer spectrum of (A) 9.9×10^{-4} M DBH plus 0.13 M AgO_2CCF_3 (—·—) and (B) 1.0×10^{-3} M DBH plus 0.13 M AgO_2CCF_3 (—·—) in methylene chloride. The absorption spectrum of the azo donor is indicated by dashed line (---) but that of 0.13 M AgO_2CCF_3 alone is not shown.

the spectral subtraction procedure precluded an accurate assessment of the absorbance, we qualitatively judge (from Figure 5) that the extinction coefficient of the high-energy band is significantly larger than that of the low-energy band delineated in

Figure 4. The separation of these absorption bands $\lambda'_{\text{CT}} = [\lambda'_{\text{CT}}(\text{DBH}-\text{Ag}^+) - \lambda'_{\text{CT}}(\text{DBO}-\text{Ag}^+)]$ is equivalent to 0.34 eV, which is essentially the same as the energy difference ($\Delta\lambda_{\text{CT}} \equiv 0.36$ eV) between CT maxima of the low-energy band shown in Figure 4

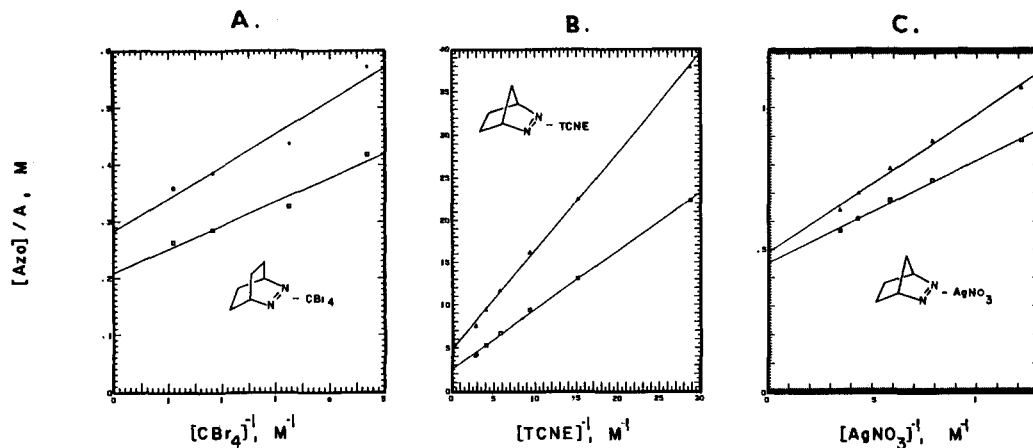
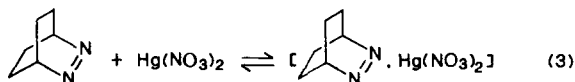


Figure 6. Spectrophotometric determination of the formation constants of the EDA complexes from (A) DBO and CBr_4 , (B) DBH and TCNE, and (C) DBH and AgNO_3 in acetonitrile at 25 °C according to the Benesi-Hildebrand method at two monitoring wavelengths.

(parts A and B). Moreover the separation is the same as the energy difference of the $n \rightarrow \pi^*$ transition in the uncomplexed azoalkanes (i.e., $\lambda_{\text{DBH}} - \lambda_{\text{DBO}} \equiv 0.35 \text{ eV}$) shown in Figure 1. The latter suggests that the high-energy bands arise from the local excitation of the azoalkane moiety in the EDA complex.²⁵ However, multiple charge-transfer can also arise in EDA complexes via the excitation from different energy levels in the electron donor or the electron acceptor or both.²⁶ The constant difference between the high- and low-energy bands in the DBO and DBH complexes strongly disfavors the last possibility and indicates that it is associated with either the azoalkane donor or the silver(I) acceptor but not both simultaneously. The photoelectron spectrum of DBO shows bands at $\text{IP}_v = 8.32$ and 10.70 eV which correspond to ionization from the HOMO (n) and the subjacent HOMO (π), respectively.¹⁴ The same CT bands in DBH occur at 8.96 and 11.53 eV .¹⁴ In other words the separation between the HOMO and SHOMO are not the same in DBO (2.38 eV) and DBH (2.57 eV), largely owing to structural differences in the internal CNN or bite angle.^{9,10} On this basis the multiple absorption bands in azoalkane-silver(I) complexes arise from excitation to the LUMO and superjacent LUMO of the electron acceptor, since it correctly predicts a constant energy difference irrespective of the structural identity of the azoalkane donor.^{1,26} Unfortunately there is insufficient evidence at this juncture to make an unequivocal choice between the alternatives. Thus we conclude that the high-energy bands in Figure 5 arise from either the local excitation of the azoalkane donor or the CT excitation to the silver(I) SLUMO. We hope that the spectral examination of other related EDA complexes will resolve this question.

The azoalkanes also form EDA complexes with a variety of other metal salts. For example, mercury(II) acetate and -nitrate afforded EDA complexes with DBO in which the well-resolved CT bands were centered at $\lambda_{\text{CT}} = 438$ and 432 nm , respectively, in acetonitrile. In the latter case, yellow-green plates of the 1:1 complex slowly crystallized from solution, and it was readily isolated in >80% yields. Similarly, when a bright blue solution



of copper(II) nitrate in acetonitrile was treated with DBO, the solution turned to an intense green. A partially resolved absorption band with a shoulder at $\sim 460 \text{ nm}$ was observed in the electronic

(25) For properties of the absorption band due to local excitation in the EDA complex, see ref 1, Chapter 3 and ref 2b, p 54 ff.

(26) (a) The LUMO in silver(I) is the 5s orbital, and the SLUMO is either the 5p or 5d orbital. (b) It is not yet established from the solution spectra (Figures 4 and 5) that the low- and high-energy bands arise from the same EDA complex. However, a comparison of these spectra with the solid-state spectra (in Nujol mull, see Experimental Section) indicates that they do despite a significant red shift of the high energy band.

Table I. Formation Constants of the EDA Complexes of Azoalkanes with Sacrificial and Inerevalent Electron Acceptors in Acetonitrile^a

donor (mM)	acceptor (mM)	λ^b (nm)	$\epsilon^{-1}_{\text{CT}}$ (M cm)	r^c	K (M^{-1})
DBO (3.0)	TCNE (57–156)	452 480	3.7×10^{-4}	0.9999	1.1
			3.5×10^{-4}	0.9996	0.85
DBO (91)	AgNO_3 (422–3020)	470	5.1×10^{-1}	0.996	1
DBO (21)	CBr_4 (213–979)	412 420	2.1×10^{-1}	0.979	5
			2.8×10^{-1}	0.969	5
DBO (1.9)	TCNE (22–138)	500	3.9×10^{-4}	0.998	3
DBH (2.6)	TCNE (35–350)	400 450	2.5×10^{-3}	0.9993	3.7
			4.8×10^{-3}	0.9994	4.2
DBN (90)	AgNO_3 (820–2920)	414 422	4.5×10^{-1}	0.997	2
			4.9×10^{-1}	0.996	2
DBN (20)	CBr_4 (210–950)	360	1.6×10^{-2}	0.974	5

^aAt 25 °C. Component in excess given as concentration range.

^bMonitoring wavelength. ^cCorrelation coefficient of Benesi-Hildebrand plot.

spectrum. Although the EDA complex were soluble in this medium, it could be isolated from a heterogeneous suspension of copper(II) nitrate in a methylene chloride solution of DBO as brilliant green microcrystals (see Experimental Section). It is interesting to note that no spectral change was detected when a green solution of copper(II) acetate in acetonitrile was exposed to DBO.

II. Formation Constants of the EDA Complexes of Azoalkanes with Sacrificial and Inerevalent Electron Acceptors in Solution. The formation constants of the azoalkane complexes with TCNE, CBr_4 , and $\text{Ag}(\text{NO}_3)_2$ were measured spectrophotometrically in acetonitrile solutions. According to the Benesi-Hildebrand method,²⁷ the concentration dependence of the absorbance of the charge-transfer band A_{CT} for a 1:1 EDA complex is given by

$$\frac{[\text{Azo}]_0}{A_{\text{CT}}} = \frac{1}{K \epsilon_{\text{CT}}} \frac{1}{[\text{Acc}]_0} + \frac{1}{\epsilon_{\text{CT}}} \quad (4)$$

under conditions in which the concentration of the electron acceptor $[\text{Acc}]_0$ is in large excess relative to the concentration of the azo donor $[\text{Azo}]_0$. K is the formation constant in eq 2, and ϵ_{CT} is the extinction coefficient at the monitoring wavelength. Typical Benesi-Hildebrand plots at two wavelengths are shown in Figure 6 for the $[\text{DBH}, \text{TCNE}]$, $[\text{DBO}, \text{CBr}_4]$, and $[\text{DBH}, \text{AgNO}_3]$ complexes. The formation constants and the extinction coefficients of these EDA complexes are listed in Table I. The formation constant of the EDA complex of DBO and tetra-cyanoethylene was also examined with the azo donor in excess (see Experimental Section).²⁸ The results in Table I indicate that

(27) Benesi, H. A.; Hildebrand, J. H. *J. Am. Chem. Soc.* **1949**, *71*, 2703.

Table II. Data Collection and Processing Parameters for X-ray Crystallography of the Azoalkane Complexes

	[(DBO) ₂ , TCNE]	[DBO, CBr ₄]	[DBO, AgNO ₃]
space group	$P\bar{1}$, triclinic	$Pmc2_1$, orthorhombic	$P2_1/c$, monoclinic
cell constants			
<i>a</i> (Å)	6.676 (2)	8.509 (3)	19.799 (5)
<i>b</i> (Å)	8.670 (6)	6.101 (2)	7.449 (4)
<i>c</i> (Å)	9.355 (5)	12.006 (6)	13.124 (9)
α (deg)	67.05 (5)		
β (deg)	75.40 (3)		106.93 (4)
δ (deg)	69.84 (4)		
<i>V</i> (Å ³)	464	623	1852
molecular formula	C ₁₈ H ₂₀ N ₈	C ₇ H ₁₀ N ₂ Br ₄	C ₆ H ₁₀ N ₃ O ₃ Ag
formula wt	348.4	441.8	280.04
formula units per cell <i>Z</i>	1	2	8
density ρ (g cm ⁻³)	1.21	2.23	2.01
absorptn coeff μ (cm ⁻¹)	0.76	127.6	21.3
radiation (Mo K α) λ (Å)	0.71073	0.71073	0.71073
collection range (deg)	4° ≤ 2 θ ≤ 50	4° ≤ 2 θ ≤ 50°	4° ≤ 2 θ ≤ 50
scan width (deg)		$\Delta\theta = (0.90 + 0.35 \tan \theta)$	
max scan time (s)	90	90	120
scan speed range (min ⁻¹)	0.9–7.0°	0.9–7.0°	0.7–5.0°
tot. data collectd	1625	682	3667
indpdnt data, <i>I</i> > 3 σ (<i>I</i>)	1343	441	2375
tot. variables	118	63	235
$R = \sum F_o - F_c / \sum F_o $	0.046	0.054	0.047
$R_w = [\sum w(F_o - F_c)^2 / \sum w F_o ^2]^{1/2}$	0.055	0.045	0.055
weights	$w = \sigma(F)^{-2}$	$w = \sigma(F)^{-2}$	$w = \sigma(F)^{-2}$

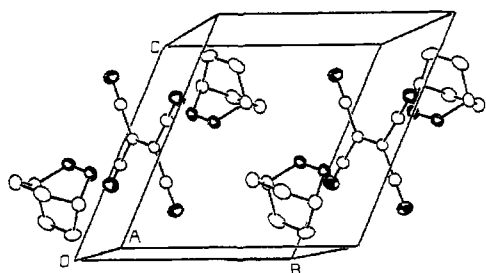


Figure 7. ORTEP diagram of the unit cell of the 2:1 EDA complex of DBO and tetracyanoethylene.

the measured value of *K* was the same under both conditions, within the experimental uncertainty of the Benesi–Hildebrand procedure.³⁰

Several features in Table I merit some discussion. First, it is important to emphasize that the quantitative comparison of the formation constants among these EDA complexes is restricted to the limitations of the Benesi–Hildebrand procedure.³⁰ Nonetheless the magnitudes of the differences in *K* are sufficient to classify all three classes of EDA complexes of azoalkanes as moderately weak.⁷ Second, the carbon tetrabromide complex of the azoalkanes is not otherwise distinguished from the tetracyanoethylene or silver(I) complexes, despite the apparent uniqueness of the charge-transfer absorption spectrum (compare Figures 2–4). Third, the uncertainty in the extrapolated extinction coefficient from the Benesi–Hildebrand intercept does not allow structural differences in the EDA complexes to be delineated.

III. Molecular Structures of the Azoalkane Complexes by X-ray Crystallography. Single crystals of the three unique classes of electron donor–acceptor complexes of azoalkanes were each grown carefully from acetonitrile solutions by the slow diffusion of diethyl ether vapor at –20 °C. The bicyclic DBO was chosen as the azo donor for the X-ray structure determinations. The pertinent crystal data and processing data for the DBO complexes with TCNE, CBr₄, and AgNO₃ are included in Table II, and the molecular

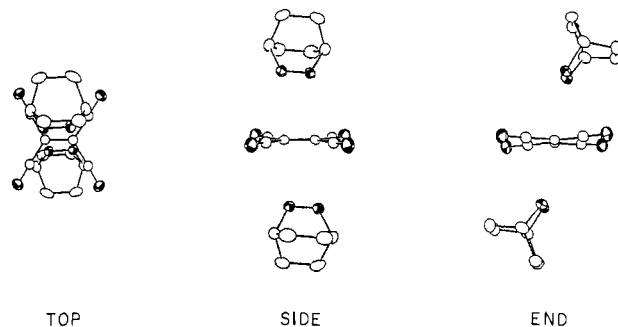


Figure 8. Orthogonal views of the CT chromophoric unit in the 2:1 EDA complex of DBO and tetracyanoethylene.

structures are described individually below.

Tetracyanoethylene. The red-orange crystal of the DBO complex with TCNE consisted of a 2:1 complex of the azo donor and the (π^*) electron acceptor. The packing in the crystal is comprised of a series of discrete EDA units each with the stoichiometry [(DBO)₂, TCNE]. The ORTEP diagram in Figure 7 illustrates the presence of two identical sandwich structures in the unit cell with a single orientation throughout. Every DBO moiety is related to another by an inversion operator (*i*) located midway between the central carbon atoms of the planar TCNE acceptor. Otherwise the bond distances of the TCNE and DBO components in Table III are essentially the same as those found in the separate acceptor and donor.³²

The charge-transfer interaction in the donor–acceptor complex of DBO and TCNE is underscored by the three perspectives shown in Figure 8. In particular the *top* and *side* perspectives locate the pairs of azo nitrogens to lie directly over the ethylenic carbon atoms in essentially colinear arrangements. Thus the azo chromophore is poised in the EDA complex to encourage the optimum CT interaction of the *n* HOMO (see Chart I) with the π^* LUMO of the TCNE acceptor. However, the slight angular displacement of the azo chromophore from the vertical position shown in the *end* perspective indicates that more than a simple HOMO–LUMO interaction of a filled *n* orbital on nitrogen with an empty π^* orbital on carbon may be involved. Indeed the tilt is consistent with a

(28) (a) Note that the relationship in eq 4 is also linear for 1:2 complexes. (b) Foster delineates the formal relationship between the measured (apparent) formation constant (Table I) and the true value for the 1:2 complex, such as in the DBO–TCNE system established by X-ray crystallography (see Figure 9).

(29) Foster, R. *Mol. Complexes* 1974, 2, 152.

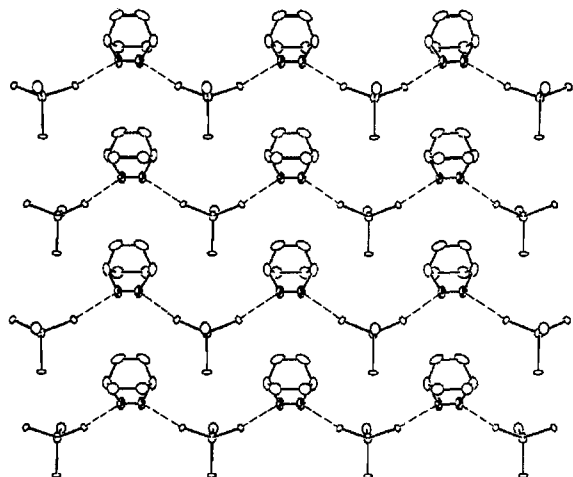
(30) For the experimental difficulty in obtaining accurate values of *K* and ϵ_{CT} for weak EDA complexes of the types examined here, see ref 31.

(31) Tamres, M.; Strong, R. L. *Mol. Assoc.* 1979, 2, 340.

(32) (a) Masnovi, J. M.; Kochi, J. K.; Hilinski, E. F.; Rentzepis, P. M. *J. Phys. Chem.* 1985, 89, 5387. (b) Harmony, J. D.; Talkington, T. L.; Nandi, R. N. *J. Mol. Struct.* 1984, 125, 125. Chiang, J. F.; Chiang, J. L.; Kratus, M. T. *J. Mol. Struct.* 1975, 26, 175.

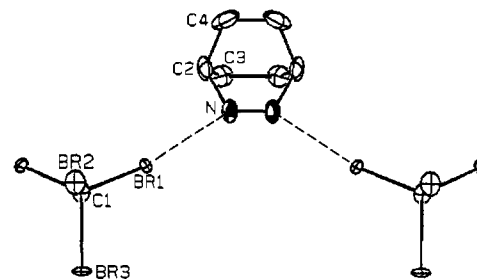
Table III. Principal Bond Distances in the DBO Complexes of TCNE, AgNO₃, and CBr₄

atom 1	atom 2	distance	atom 1	atom 2	distance	atom 1	atom 2	distance
[(DBO) ₂ , TCNE]								
N1	C3	1.137 (1)	C1	C1	1.343 (1)	C5	C6	1.519 (1)
N2	C2	1.136 (1)	C1	C2	1.434 (1)	C6	C7	1.513 (1)
N3	N4	1.236 (1)	C1	C3	1.431 (1)	C7	C8	1.513 (1)
N3	C4	1.475 (1)	C4	C5	1.514 (1)	C8	C9	1.514 (1)
N4	C7	1.470 (1)	C4	C9	1.513 (1)			
[DBO, AgNO ₃]								
Ag	O1	2.650 (3)	C1	C5	1.536 (6)	O1'	N1'	1.233 (4)
Ag	O1	2.487 (3)	C1	C7	1.522 (6)	O2'	N1'	1.226 (4)
Ag	O2	2.754 (3)	C4	C6	1.517 (5)	O3'	N1'	1.206 (4)
Ag	O3	2.599 (3)	C4	C8	1.523 (6)	N2'	N3'	1.258 (3)
Ag	N2	2.297 (3)	C5	C6	1.519 (6)	N2'	C1'	1.467 (4)
Ag	N3	2.270 (3)	C7	C8	1.496 (6)	N3'	C4'	1.477 (4)
O1	N1	1.228 (4)	Ag'	O1'	2.574 (3)	C1'	C5'	1.507 (6)
O2	N1	1.224 (3)	Ag'	O1'	2.555 (2)	C1'	C7'	1.537 (6)
O3	N1	1.233 (4)	Ag'	O2'	2.517 (3)	C4'	C6'	1.522 (5)
N2	N3	1.246 (3)	Ag'	O3'	2.917 (3)	C4'	C8'	1.511 (5)
N2	C1	1.456 (4)	Ag'	N2'	2.273 (3)	C5'	C6'	1.531 (6)
N3	C4	1.472 (4)	Ag'	N3'	2.301 (3)	C7'	C8'	1.527 (6)
[DBO, CBr ₄]								
C1	Br1	1.938 (9)	N	N	1.11 (2)	C2	C4	1.49 (2)
C1	Br2	1.79 (2)	N	C2	1.53 (2)	C3	C3	1.56 (5)
C1	Br3	2.04 (2)	C2	C3	1.43 (3)	C4	C4	1.35 (5)

**Figure 9.** Molecular structure of the 1:1 EDA complex of DBO and carbon tetrabromide showing the alternating series of continuous, one-dimensional CT interactions.

secondary CT interaction of the filled azo π orbital (see Chart I) with the symmetric combination of the empty π^* orbitals of the 1,2-cyano groups. Be that as it may, the molecular structure of [(DBO)₂, TCNE] in Figure 7 does not support the usual CT interaction of a donor π orbital with the π^* orbital of TCNE, as commonly encountered in other EDA complexes of this ubiquitous electron acceptor.³³

Carbon Tetrabromide. The pale yellow crystal from DBO and CBr₄ consisted of a 1:1 complex of the azo donor and the (σ^*) electron acceptor. The ORTEP diagram in Figure 9 shows the packing in the crystal to be comprised of a series of sinuous chains of alternating molecular associations of the DBO donor and the CBr₄ acceptor. Each chain is propagated by a series of mirror planes passing perpendicularly through the N=N linkage (or through CBr₄). Figure 9 also illustrates the manner in which the infinite one-dimensional polymers stack in uniform columns of the donor and acceptor but with an up/down sense to the DBO moieties. Indeed the different chains are crystallographically related by a perpendicular 2₁ screw axis which directly transforms

**Figure 10.** Isolated unit of the CT chromophore in the 1:1 EDA complex of DBO and carbon tetrabromide showing both bridging "bromine bonds" to the azo linkage.

one chain into its immediate neighbor.

Every molecule of carbon tetrabromide uses a pair of bromine atoms to serve as bridges to the contiguous azoalkanes. Each molecule of DBO is thus formally associated with a pair of CBr₄ molecules at each nitrogen center to form essentially a doubly bridged entity. Moreover the pair of bridging bromines are thermally constrained, as indicated by their relatively small root-mean-square amplitudes for thermal vibration. By contrast the other pair of bromines having no close contacts with DBO show relatively large thermal ellipsoids in Figure 9. Otherwise the bond distances of the CBr₄ and DBO components in Table III are essentially the same as those found in the separate acceptor and donor.^{32b,34}

Indeed the charge-transfer interaction in the donor-acceptor complex of DBO and CBr₄ is contained in each chromophoric C-Br...N unit shown in isolation by Figure 10. The more or less linear C-Br...N arrangement encourages the optimum CT interaction of the n HOMO on the nitrogen atom with the σ^* LUMO of the Br-C bond. The relevant Br...N bond distance of 2.91 Å is only slightly longer than that found in the EDA complex of carbon tetrabromide with such tertiary amines as dabco (2.88 and 2.76 Å) and quinuclidine (2.53 Å),³⁵ but it is significantly shorter than the sum of the van der Waals radii of 3.5 Å. The CT interactions to the pair of CBr₄'s located at both ends of the azo linkage are coplanar, the dihedral angle described by the

(33) (a) Melby, L. R. *Chemistry of the Cyano Group*; Rapport, Z., Ed.; Wiley: 1970, p 639 ff. (b) Herbstein, F. H. *Persp. Struct. Chem.* **1971**, *4*, 169. (c) Prout, C. K.; Kamenar, B. *Mol. Complexes* **1973**, *1*, 151.

(34) More, M.; Baert, F.; Lefebvre, J. *Acta Crystallogr., Sect. B: Struct. Crystallogr. Cryst. Chem.* **1977**, *B33*, 3681. See, also: More, M.; Lefebvre, J.; Fouret, R. *Acta Crystallogr., Sect. B: Struct. Crystallogr. Cryst. Chem.* **1977**, *B33*, 3862.

(35) Blackstock, S. C.; Lorand, J. P.; Kochi, J. K. *J. Org. Chem.*, in press.

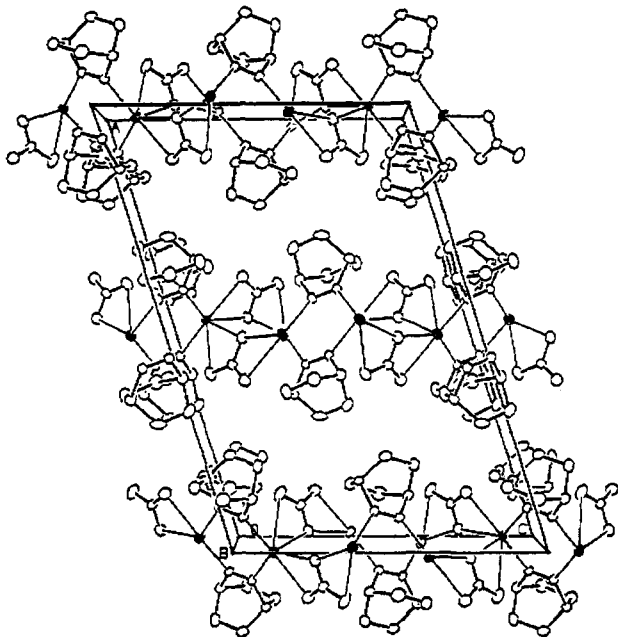


Figure 11. ORTEP diagram of the unit cell of the 1:1 EDA complex of DBO and silver(I) nitrate from the edge perspective of the infinite two-dimensional sheets of the dimeric $[(\text{DBO})_2, (\text{AgNO}_3)_2]$ network.

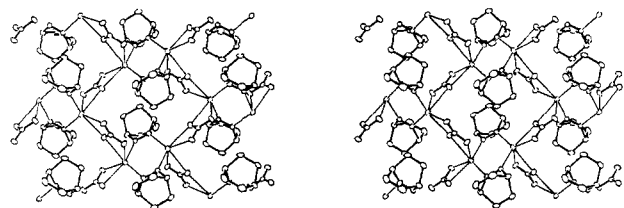


Figure 12. Stereoscopic view from the top of the infinite, two-dimensional network of dimeric $[(\text{DBO})_2, (\text{AgNO}_3)_2]$ units.

nonbonded close contacts $\text{Br}\cdots\text{N}=\text{N}\cdots\text{Br}$ being 0° , as dictated by the presence of the crystallographic mirror plane (vide supra).

Silver(I) Nitrate. The canary yellow crystal from DBO and AgNO_3 consisted of a 1:1 complex of the azo donor and the (ν) electron acceptor. The packing in the crystal is comprised of a series of two-dimensional layers of an infinite network of interconnected units of DBO and silver nitrate. The ORTEP diagram of the unit cell in Figure 11 presents the edge perspective of two different layers which occur in an alternating sequence. Although the two layers are crystallographically independent, they contain the same basic connectivities of DBO to AgNO_3 . Thus each layer has silver(I) atoms which are always six-coordinate to a pair of η^2 -nitrate and two DBO ligands. Each nitrate is tetrahapto overall, being simultaneously bound to two silver(I) atoms. Every DBO serves as a σ -donor ligand to two silver(I) atoms. The stereoscopic view from the top of the infinite two-dimensional network is presented in Figure 12.

The charge-transfer interaction in the donor-acceptor complex of DBO and AgNO_3 is contained within a dimeric chromophoric unit of stoichiometry $[(\text{DBO})_2, (\text{AgNO}_3)_2]$. The relevant silver(I)-azo interaction is included in the six-membered ring shown in isolation by Figure 13. The $\text{Ag}-\text{N}$ bond distances of 2.30 and 2.27 Å from a particular azo donor are slightly longer than that previously observed (2.21 Å) in the silver(I) nitrate complex with the heteroaromatic pyrazine.³⁶ Similarly the $\text{Ag}-\text{O}$ bond distances to the bidentate nitrate ligands are somewhat shorter. However the nitrate ligand is not critical to the charge-transfer interaction in the EDA complexes since we found the trifluoroacetato, toluenesulfonato, and trifluoromethanesulfonato derivatives of silver(I) to be spectroscopically undistinguished from silver(I) nitrate. Such oxy ligands thus merely serve as multiple bridges

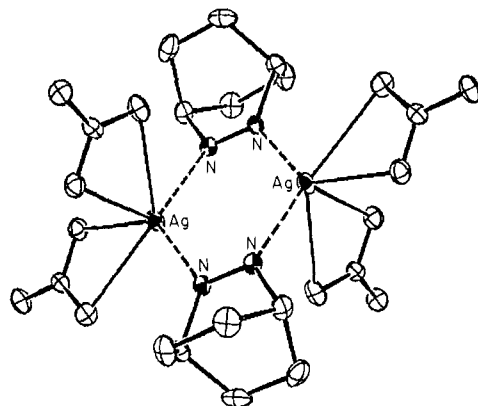
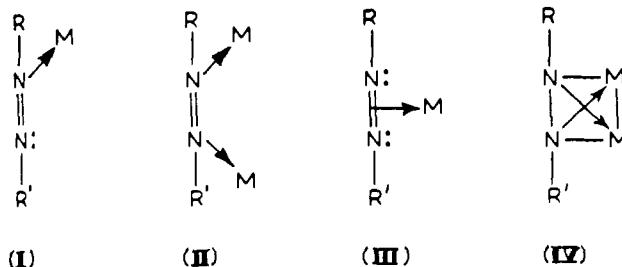


Figure 13. ORTEP diagram of the CT chromophore in the dimeric unit of the 1:1 EDA complex of DBO and silver(I) nitrate.

to bind the critical silver(I)-azo chromophores in an infinite, two-dimensional array. The six-membered chromophoric unit exists in a nonplanar, boatlike conformation. There is a crystallographic inversion operator in the center of the hexagon, with the silver atoms situated at a flap angle of $19 \pm 0.3^\circ$.³⁷ Such a conformation results in a distortion of the azo n orbitals from a torsion angle of 0° in the uncomplexed donor to 22° in the silver(I) complex. However the skeletal framework of DBO is relatively unaffected, the increase in the internal dihedral angle $\text{C}-\text{N}=\text{N}-\text{C}$ from 0° to $1.9 \pm 0.3^\circ$ being within 6σ . The principal bond lengths in the EDA complex with silver(I) nitrate are included in Table III.

Formally the EDA complex of DBO and AgNO_3 is related to a large class of coordination compounds, particularly of transition metals.³⁸ The azo ligands in the latter are bound sufficiently strongly that the metal moiety (M) generally does not exist independently in reversible equilibrium.³⁹ A rich variety of coordination modes involving one (I) or both (II) nitrogen lone pairs, the π bond (III), and all three (IV) orbitals are known.^{39,40} In



these coordination compounds, except for intramolecular ($L \rightarrow M$ or $L \leftarrow M$) absorptions, we know of no examples in which (intermolecular) CT bands of the kind described here have been reported. It is possible however that the latter are precursors (and may exist as preequilibrium encounter complexes) in the ultimate formation of the strongly bound, intimate coordination complexes I-IV. We hope that the charge-transfer photochemistry of the type introduced in the following section will serve to delineate these interesting differences further.

IV. Charge-Transfer Excitation of the Azo Complexes with Sacrificial and Inequivalent Electron Acceptors. Comments on the Radical Cations of Azoalkane Donors. The photoexcitation of the charge-transfer bands of the EDA complexes of azoalkane donors was examined qualitatively by irradiating solutions of DBO in acetonitrile containing either TCNE, iodine, silver(I) nitrate, and trifluoroacetate or perfluoroalkyl radical as electron acceptors.

(37) The silver atoms are displaced 0.37 Å above and below the plane described by the two azo linkages.

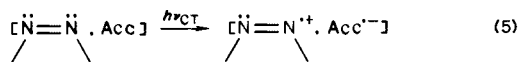
(38) Bruce, M. I.; Goodall, B. L. In *Chemistry of the Hydrazo, Azo and Azoxy Groups*; Patai, S., Ed.; Wiley: 1975; Part I, Chapter 9.

(39) (a) Kilner, M. *Adv. Organomet. Chem.* **1972**, *10*, 115. (b) Carty, A. *J. Organomet. Chem. Rev.* **1972**, *A7*, 191.

(40) Ackerman, M. N.; Kou, L.-J.; Richter, J. M.; Willet, R. M. *Inorg. Chem.* **1977**, *16*, 1298. Ackerman, M. N.; Kou, L.-J. *J. Organomet. Chem.* **1975**, *86*, C7; *Inorg. Chem.* **1976**, *15*, 1423.

In order to ensure that only the charge-transfer band was excited in each case, the actinic output from a 1-kW high-pressure mercury lamp was passed as a focussed beam through Corning sharp cutoff filters which allowed only light with wavelength (usually $\lambda > 400$ nm) beyond the CT maximum to impinge on the photochemical cell. The photochemical change accompanying the CT excitation was monitored by following the decrease in the CT absorbance and/or the ^1H NMR spectrum of the azo donor (vide supra). Even after irradiation for an hour or so, no change was observed. The DBH complexes with TCNE and AgNO_3 were also equally unreactive to the irradiation of the CT bands. However, the CT irradiation of the EDA complexes of DBO with carbon tetrabromide, mercury(II) acetate, and tetranitromethane led to rather rapid changes in both the absorption spectra and the ^1H NMR spectra. Thus the development of strong new absorptions at $\lambda > 450$ nm together with the simultaneous appearance of a number of new resonances generally characterized the photoexcitation of these EDA complexes. Although the spectral alterations were too complex for identification at this point, the magnitudes of the changes point to the occurrence of CT processes with sizeable quantum yields.

The difference in the photochemical responses of the azo complexes with the two sets of electron acceptors may be qualitatively accounted for in the following way. The time-resolved spectroscopic studies have established the donor-acceptor ion pair as the CT excited state.⁴¹⁻⁴³ As applied to the bicyclic azo complexes of importance to this study, the relevant CT excitation from the EDA complex can thus be depicted as



in which Acc is an electron acceptor. Such a formulation focuses on the azo cation-acceptor anion as the CT excited ion pair. This ion pair can suffer several fates, among which are (a) back electron transfer to regenerate the original EDA complex, (b) diffusive separation to the free azo cation-radical and the acceptor anion-radical, and (c) irreversible decomposition via a unimolecular fragmentation of azo cation-radical and/or the acceptor anion-radical. Each of these dynamic processes has been described.⁴¹⁻⁴³ Since diffusive separation of the ion pair (b) generally cannot compete with back electron transfer (a), the principal course of the CT photochemistry usually derives from the fragmentation route (c). Indeed of the various electron acceptors cited above, only carbon tetrabromide, tetranitromethane, and mercury(II) acetate are known to undergo facile dissociative electron attachment.⁴⁴⁻⁴⁶ The other acceptors such as tetracyanoethylene, silver(I), and perfluoroalkyl radical yield relatively more persistent anion-radicals.⁴⁷ We hope that product analyses will identify these pathways for decomposition of the acceptor anion-radicals at a later time. On the other hand, the properties of the azo cation-radical are less well-described. Although azobenzene cation-radical has been tentatively identified,⁴⁸ the alkyl analogues are unknown. Recent studies of the chemical oxidation of 1,1'-azoadamantane by thianthrene cation suggest that the cation

(41) Hilinski, E. F.; Masnovi, J. M.; Amatore, C.; Kochi, J. K.; Rentzepis, P. M. *J. Am. Chem. Soc.* **1983**, *105*, 6167. Hilinski, E. F.; Masnovi, J. M.; Kochi, J. K.; Rentzepis, P. M. *J. Am. Chem. Soc.* **1984**, *106*, 8071.

(42) Masnovi, J. M.; Huffman, J. C.; Kochi, J. K.; Hilinski, E. F.; Rentzepis, P. M. *Chem. Phys. Lett.* **1984**, *106*, 20. Masnovi, J. M.; Kochi, J. K.; Hilinski, E. F.; Rentzepis, P. M. *J. Am. Chem. Soc.* **1986**, *108*, 1126.

(43) Masnovi, J. M.; Kochi, J. K. *J. Am. Chem. Soc.* **1985**, *107*, 6781.

(44) Compare Gaines, A. F.; Kay, J.; Page, F. M. *Trans. Faraday Soc.* **1966**, *62*, 874. Illenberger, E. *Ber. Bunsen. Phys. Chem.* **1982**, *86*, 252. Hamill, W. H.; Guarino, J. P.; Ronayne, M. R.; Ward, J. A. *Disc. Faraday Soc.* **1963**, *36*, 169.

(45) Bielski, B. H. J.; Allen, A. O. *J. Phys. Chem.* **1967**, *71*, 4544. Rabani, J.; Mulac, W. A.; Matheson, M. S. *J. Phys. Chem.* **1965**, *69*, 53. Chaudhuri, S. A.; Asmus, K. D. *J. Phys. Chem.* **1972**, *76*, 26.

(46) Cf. Lau, W.; Kochi, J. K. *J. Org. Chem.* **1986**, *51*, 1801.

(47) (a) Webster, O. W.; Mahler, W.; Benson, R. E. *J. Am. Chem. Soc.* **1982**, *84*, 3678. (b) Compare Gee, D. R.; Russell, K. E.; Wan, J. K. S. *Can. J. Chem.* **1971**, *49*, 160; **1970**, *48*, 2740; *J. Chem. Phys.* **1970**, *53*, 847.

(48) Bargon, J.; Seifert, K. G. *Tetrahedron Lett.* **1974**, 2265.

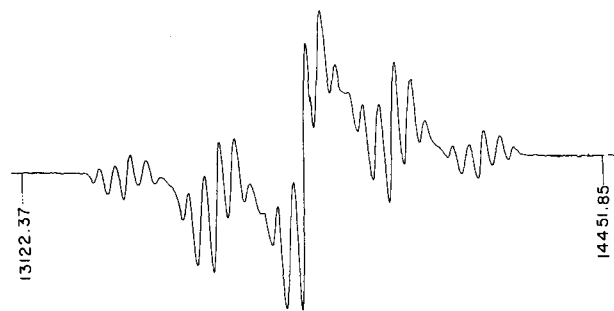
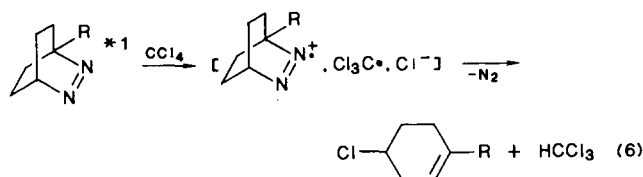
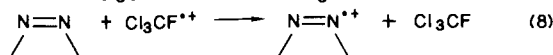
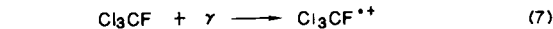


Figure 14. ESR spectrum obtained at 140 K from the γ -radiolysis of a dilute matrix of $\sim 10^{-2}$ M DBH in Cl_3CF at 77 K. Proton NMR field markers are in kHz.

radical is labile and undergoes rapid loss of nitrogen.⁴⁹ More pertinent to CT excited states of the EDA complexes described here, the quenching of the fluorescence of various substituted diazabicyclooctenes by carbon tetrachloride has been ascribed to an electron-transfer process,⁵⁰ i.e.

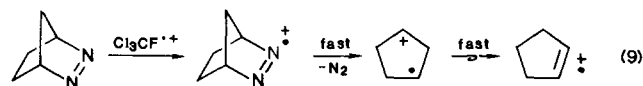


In order to examine directly the properties of the azo cation-radicals, we applied the freon matrix technique for the production and the ESR observation of cation-radicals.⁵¹ In this method, the inert fluorocarbon Cl_3CF is employed both as a rigid matrix and a powerful chemical oxidant which is generated during the γ -radiolysis of a dilute frozen solution of the donor at 77 K, e.g.,



Since Cl_3CF melts at 162 K, the system provides a sizeable thermal window to examine the effects of temperature on the ESR spectra of cation-radicals.

When a sealed, suprasil tube containing a 0.01 M solution of DBH in Cl_3CF was cooled to 77 K, it formed a colorless opaque glass which was γ -irradiated to a dose of $\sim 10^6$ rad. The somewhat broadened ESR spectrum of the irradiated mixture taken at 140 K is shown in Figure 14. The principal feature of the spectrum ($g = 2.00269$) is readily seen to consist of a large quintet splitting of $a_{\text{H}} = 50$ G with a binomial intensity ratio; each line is further split further into small quintet splittings of $a_{\text{H}} = 7$ G. The ESR spectrum is identical with that obtained earlier from cyclopentene.⁵² Indeed INDO calculations predict cyclopentene cation-radical to show large splittings of 50.4 G for the four β -methylene protons adjacent to the double bond and the accidental equivalency of the pairs of γ -methylene protons (7.0 G) and α -alkenyl protons (7.1 G). Such an unambiguous structural assignment suggests that the DBH cation-radical is prone to the ready loss of dinitrogen. The subsequent rearrangement is known to be rapid even at 4 K,⁵³ i.e.



We conclude from this study that the barrier to the loss of di-

(49) Bae, D. H.; Engel, P. S.; Hogue, A. K. M. M.; Keys, D. E.; Lee, W.-K.; Shaw, R. W.; Shine, H. J. *J. Am. Chem. Soc.* **1985**, *107*, 2561.

(50) Engel, P. S.; Keys, D. E.; Kitamura, A. *J. Am. Chem. Soc.* **1985**, *107*, 4964.

(51) Shida, T.; Kato, T. *Chem. Phys. Lett.* **1979**, *68*, 106. Shida, T.; Haselbach, E.; Bally, T. *Acc. Chem. Res.* **1984**, *17*, 180.

(52) Shida, T.; Egawa, Y.; Kubodera, H.; Kato, T. *J. Chem. Phys.* **1980**, *73*, 5963.

(53) Ushida, K.; Shida, T.; Walton, J. C. *J. Am. Chem. Soc.* **1986**, *108*, 2805.

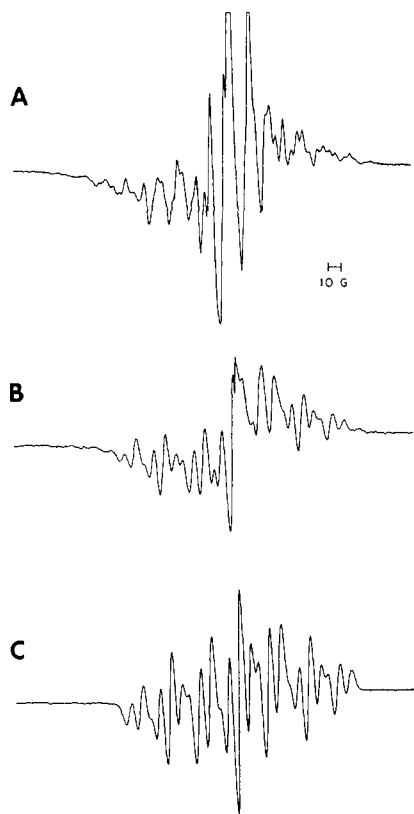
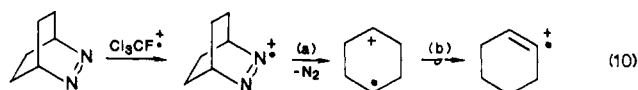


Figure 15. ESR spectra obtained at 140 K from (A) the γ -radiolysis of a dilute matrix of $\sim 10^{-2}$ M DBO in Cl_3CF at 77 K and (B) after photobleaching of A with blue light ($\lambda > 415$ nm). (C) ESR spectrum of cyclohexene cation radical at 140 K from the γ -radiolysis of cyclohexene in Cl_3CF at 77 K according to Shida et al.⁵²

nitrogen from DBH cation-radical is less than 5 Kcal mol⁻¹, since it apparently has a lifetime of under 10 min at 77 K.

The spectral assignment of the intermediate(s) following the formation of the homologous DBO cation-radical is less clear. Thus a dilute Cl_3CF matrix of DBO was γ -irradiated at 77 K, and the ESR spectrum of the resultant mixture measured at 140 K is shown in Figure 15A. The careful examination of this unsymmetrical ESR spectrum indicates that it either derives from a mixture of radicals with slightly different g values or contains anisotropic components.⁵⁴ Interestingly, this ESR spectrum persists up to the melting temperature of the matrix. However if the matrix is irradiated with blue light ($\lambda > 415$ nm) at 140 K, the ESR spectrum is efficiently converted to that shown in Figure 15B. The principal features of the ESR spectrum in Figure 15B coincide with those in Figure 15C of the cyclohexene cation radical,⁵² i.e.



[The latter was generated under the same radiolytic conditions from cyclohexene.] We thus conclude that the nitrogen loss (step a) and/or rearrangement (step b) following the formation of DBO cation-radical are (is) less facile than in the more highly strained DBH analogue.⁵⁵

These ESR studies support the qualitative conclusion that azoalkane cation-radicals are labile. However the CT photochemical studies indicate that the cation-radicals formed in eq 5 are not so unstable as to preclude back electron transfer—especially from those persistent acceptor anion-radicals derived from tetracyanoethylene, chloranil, perfluoroalkyl radical, etc.

(54) Note that the ESR spectra in Figure 15A is not symmetrical. For further discussion of its structural assignment, see Experimental Section.

(55) For steric strain in DBO, DBH, and azo compounds generally, see: Harmony and co-workers in ref 32b and Engel in ref 50.

Only those electron acceptors which afford highly transient anion-radicals are able to effectively promote charge-transfer photochemistry. We hope that time-resolved spectroscopy will allow us to examine the cation-radicals of azoalkanes produced from the charge-transfer excitation of the EDA complexes with the various electron acceptors described in this study.⁵⁶

Summary and Conclusions

Azoalkanes are versatile electron acceptors capable of forming a wide variety of electron donor-acceptor complexes with unique structures. These molecular associations are characterized by the appearance of striking colors characteristic of intermolecular charge-transfer bands according to Mulliken theory. Accordingly, the formation constants K of the EDA complexes in solution are dependent on the donor properties of the azoalkane as measured by their vertical ionization potential.

The isolation of single crystals of the EDA complexes of azoalkanes with TCNE, CBr_4 , and AgNO_3 allows the X-ray crystallographic determination of the molecular structures to be derived from three classes of sacrificial and inerevalent electron acceptors. The structures of the complexes follow from the symmetry of the HOMO-LUMO interaction. Thus Figure 8 relates the filled antisymmetric n -orbital (Chart I) of the azo donor to the empty π^* orbital of the TCNE acceptor to form discrete 2:1 EDA units (Figure 7). Figure 10 emphasizes the bridging nature of the "bromine bond" derived from the filled n orbital of the azo donor and the empty σ^* orbital of the CBr_4 acceptor to generate an infinite one-dimensional chain (Figure 9). Figure 13 pertains to the empty 5s orbital on silver(I) with the n azo orbitals which generates dimeric hexagonal units interconnected into infinite, two-dimensional layers (Figure 12). The charge-transfer excitation in such two-dimensional polymers should confer interesting electrical properties in the solid state. Indeed the selective charge-transfer photochemistry of azo complexes observed with some electron acceptors but not others relate to the behavior of the CT excited ion pair. The relevance of the azo cation radical in the latter can be examined by matrix isolation and ESR spectroscopy.

In a more general context, we believe that molecular associations of electron donors and acceptors are crucial to an understanding of reaction dynamics of nucleophiles and electrophiles.⁶ This study shows that the spectral characterization of even weak donor-acceptor interactions in solution can be elucidated by the isolation of crystalline molecular complexes and the establishment of their structures by X-ray crystallography. However, we hasten to add the caveat that such a direct interrelationship must be pursued with a degree of caution. For example, the ready crystallization of the 2:1 complex of DBO and tetracyanoethylene belies the apparent predominance of the 1:1 complex in solution as simply evaluated by the Benesi-Hildebrand method. Although a variety of EDA complexes with different stoichiometries may be extant in solution, clearly factors other than their relative formation energies are involved as to which complex crystallizes preferentially from solution. Nonetheless the X-ray structure of the 2:1 complex undoubtedly delineates the essential geometrical requirement for the HOMO-LUMO interaction that is also common to the 1:1 complex.

Experimental Section

Materials. DBO (2,3-diazabicyclo[2.2.2]octene) and DBH (2,3-diazabicyclo[2.2.1]hept-2-ene) were prepared from the Diels-Alder reaction of diethyl azodicarboxylate with 1,3-cyclohexadiene and cyclopentadiene, respectively.^{14,22,23} AB (*trans*-azo-2-butane) was obtained from Merck, Sharpe and Dohme of Canada and used as such. AIBN (*trans*-azo-2-cyano-2-propane) from DuPont was repeatedly recrystallized from ethanol until colorless prior to use. Carbon tetrabromide and tetracyanoethylene (Aldrich) were purified by sublimation several times until colorless. Silver(I) nitrate (ACS crystals from D. F. Goldsmith Chemical and Metal Corp.) was used without further purification. Silver(I) trifluoroacetate, *p*-toluenesulfonate, and trifluoromethanesulfonate were materials prepared and purified in a previous study. Chloranil (Aldrich),

(56) Compare Masnovi, J. M.; Kochi, J. K. *J. Am. Chem. Soc.* **1985**, *107*, 7880.

mercury(II) acetate (Baker), mercury(II) nitrate (G. F. Smith), copper(II) acetate (Baker), and copper(II) nitrate (Mallinckrodt) were used without further purification. Tetranitromethane was used without further purification. Tetranitromethane was prepared from the nitration of acetic anhydride.⁵⁷ Perfluoroalkyl radical (perfluoro-2,4-dimethyl-3-ethyl-3-pentyl radical) was kindly supplied to us as a colorless liquid by K. V. Scherer.¹⁸ Trichlorofluoromethane (freon II) from Aldrich was redistilled from phosphorus pentoxide under an argon atmosphere. Acetonitrile (Burdick and Jackson, UV grade) and methylene chloride (Aldrich, gold label) were used without further purification.

Crystalline EDA complexes of the azoalkanes were prepared as follows.

[DBO, AgNO₃]. DBO (20.8 mg, 0.19 mmol) and AgNO₃ (37 mg, 0.22 mmol) were mixed in 1 mL of acetonitrile. The resulting yellow solution was cooled to -20 °C under an atmosphere saturated with diethyl ether in the dark. After 24 h, dark yellow crystals (46 mg) were recovered (87%): IR (KBr) 2869 (w), 2427 (w), 2396 (w), 1385 (s), 824 (m) cm⁻¹; ¹H NMR (CD₃CN) δ 4.99 (br s, 2 H), 1.0–1.75 (m, 8 H) for 0.4 M DBO and δ 5.12 (br s, 2 H), 1.1–1.8 (m, 8 H) for 0.4 M DBO plus 0.36 M AgNO₃; UV-vis (Nujol mull) very broad absorption λ_{CT} = 397–9 nm.

[DBH, AgNO₃]. DBH (29 mg, 0.31 mmol) and AgNO₃ (56 mg, 0.33 mmol) were mixed in 1 mL of acetonitrile. The resulting solution was treated as described above to yield 72 mg (88%) of light yellow crystals: IR (KBr) 2479 (w), 2426 (w), 2395 (w), 1383 (s), 1764 (w), 8.26 (m) cm⁻¹. ¹H NMR (CD₃CN) δ 5.06 (s, 2 H), 1.4–1.65 (m, 2 H), 1.12 (q, 2 H), 0.65–0.9 (m, 2 H) for 0.36 M DBH and δ 5.15 (s, 2 H), 1.5–1.75 (m, 2 H), 1.23 (m, 2 H), 0.7–1.0 (m, 2 H) for 0.36 M DBH plus 0.36 M AgNO₃; UV-vis (Nujol mull) very broad absorption λ_{CT} = 376–9 nm. Anal. Calcd for C₅H₈N₃O₃Ag: C, 22.57; H, 3.04; N, 15.80. Found: C, 22.47; H, 3.08; N, 15.76.⁵⁸

[DBO, CBr₄]. DBO (52 mg, 0.48 mmol) was mixed with CBr₄ (211 mg, 0.64 mmol) in 1.5 mL of acetonitrile. After initial dissolution at room temperature, the yellow solution slowly deposited pale yellow crystals (80 mg). Cooling the supernatant mother liquors afforded an additional 90 mg (81% total). IR (KBr) 2866 (m), 1520 (m), 1463 (m), 1448 (w), 1320 (w), 1235 (w), 1167 (w), 1138 (2), 1098 (w), 1024 (2), 891 (w), 822 (w), 794 (w), 671 (s) cm⁻¹; ¹H NMR (CD₃CN) δ 5.00 (s, 2 H), 1.0–1.75 (m, 8 H) for 0.28 M DBO plus 0.21 M CBr₄. Anal. Calcd for C₇H₁₀N₂Br₄: C, 19.03; H, 2.29; N, 6.34. Found: C, 19.10; H, 2.30; N, 6.31.

[DBH, CBr₄]. DBH (43 mg, 0.44 mmol) was mixed with CBr₄ (156 mg, 0.47 mmol) in 1 mL of acetonitrile to give an almost colorless solution. After having been cooled to -20 °C in the dark, the solution deposited pale yellow-green plates (121 mg, 63%). IR (KBr) 3013 (w), 2997 (w), 1276 (m), 1253 (w), 1195 (w), 1121 (m), 1008 (w), 974 (w), 947 (w), 881 (w), 838 (w), 819 (w), 675 (s) cm⁻¹; ¹H NMR (CD₃CN) δ 5.06 (s, 2 H), 1.4–1.65 (m, 2 H), 1.12 (q, 2 H), 0.65–0.9 (m, 2 H). Anal. Calcd for C₆H₈N₂Br₄: C, 16.84; H, 1.89; N, 6.55. Found: C, 17.03; H, 1.94; N, 6.62.

(DBO, TCNE). TCNE (69 mg, 0.54 mmol) was added to a 5-mL, round-bottomed flask and charged with DBO (58 mg, 0.53 mmol) in 2 mL of acetonitrile. The resulting deep red-brown solution was placed under an argon atmosphere, allowed to stand at room temperature for 1 h, and then cooled to -20 °C in the dark. After 24 h, the large dark red-brown crystals were collected at -20 °C by removing the supernatant solution via a 22-gauge Teflon cannula. The solution was reduced in volume by 50%, cooled to -20 °C and a second crop of crystals were collected (62 mg, 50%). IR (KBr) 2259 (w), 2247 (w), 2203 (w), 2177 (w), 1520 (s), 1462 (w), 1455 (s), 1351 (w), 1332 (w), 1323 (s), 1256 (w), 1240 (m), 1159 (s), 1138 (w), 1099 (m), 1049 (w), 1030 (m), 1023 (m), 963 (w), 942 (w), 912 (w), 889 (m), 819 (m), 794 (m), 657 (w), 577 (w), 542 (w); ¹H NMR (CD₃CN) δ 5.03 (s, 2 H), 1.0–1.8 (m, 8 H) from 0.21 M DBO plus 0.22 M TCNE; UV-vis (Nujol mull) very broad absorption, λ_{CT} = 356–8, 424–8, 540–5 (sh). Elemental Anal. Calcd for C₁₈H₂₀N₈: C, 62.05; H, 5.79; N, 32.16. Found: C, 61.01; H, 5.77; N, 32.47. **[DBO, Hg(NO₃)₂].** DBO (55 mg, 0.50 mmol) was mixed with Hg(NO₃)₂ (294 mg, 0.86 mmol) in 5 mL of acetonitrile. Immediately upon mixing, a yellow-green solid precipitated. Additional solid slowly precipitated as the solution was allowed to stand for an additional hour. When the supernatant liquor was cooled to -20 °C, an additional yellow-green plate crystallized (146 mg, 68% total) [Elemental Anal. Calcd for C₆H₁₀N₄O₆Hg: C, 16.57; H, 2.32; N, 12.89. Found: C, 16.56; H, 2.32; N, 12.86]. **[DBO, Cu(NO₃)₂].** To a solution of DBO (10 mg, 0.09 mmol) in 2 mL of methylene chloride was added 1 equiv of Cu(NO₃)₂ as crystals. The copper(II) salt alone was insoluble in methylene chloride, but the continuous stirring of the mixture caused the liquid phase to turn

Table IV. Spectrophotometric Determination of the Formation Constant of the EDA Complex of DBO and TCNE^a

DBO (M)	TCNE (M)	A ₄₅₂	A ₄₈₀
0.00300	0		
0.00300	0.0566	0.462	0.400
0.00300	0.0922	0.726	0.636
0.00300	0.111	0.865	0.761
0.00300	0.136	1.02	0.902
0.00300	0.156	1.14	1.01
DBO (M)	TCNE (M)	A ₄₅₀	A ₅₀₀
0	0.00195	0.003	0.001
0.0218	0.00195	0.158	0.100
0.0541	0.00195	0.321	0.248
0.0809	0.00195	0.448	0.307
0.110	0.00195	0.576	0.397
0.138	0.00195	0.692	0.486

^a In acetonitrile at 25 °C.

bright green. The solution was filtered to remove the insoluble Cu(N-O₃)₂, and it was cooled to -20 °C under an atmosphere of diethyl ether in the dark. After several days intensely green microcrystals were deposited. Elemental Anal. Calcd for C₆H₁₂N₄O₇Cu·H₂O: C, 22.82; H, 3.83; N, 17.74. Found: C, 23.35; H, 4.09; N, 16.84.

Instrumentation. The UV-vis absorption spectra were measured on a Hewlett-Packard 8450A diode array spectrophotometer with 2-cm⁻¹ resolution. The ¹H and ¹³C NMR spectra in solution were obtained on a JEOL FX 90Q FT NMR spectrometer. The ESR spectra were recorded on a Varian E-112 Q-band spectrometer equipped with a ¹H NMR gaussmeter for field calibration. The γ-radiolysis was carried out with a ⁶⁰Co source (gamma cell 220, Atomic Energy of Canada) with an output of 1 × 10⁶ rad h⁻¹. The light source for all vis irradiations consisted of a focussed beam for either a Optometric (no. XBO450) 450-W xenon lamp or a Hanovia (no. 977-B1) 1000-W high pressure mercury/xenon lamp. Glass sharp cutoff filters (Corning) were used to eliminate light with wavelengths less than that of the CT bands.

Determination of the Formation Constants. In a typical study, a 2-mL aliquot of a standard solution of the azoalkane was transferred to a 1-cm precision quartz cell equipped with a magnetic stir bar. All spectra were measured relative to the pure solvent as reference. Successive additions of a preweighed amount of the appropriate electron acceptor to the solution was followed by thorough stirring. The volume change attendant upon the addition of the latter was assumed to be negligible. After the final spectrum was measured, it was allowed to stand for ~10 min as a check for stability. A spectra of the azoalkane and the electron acceptor at their highest concentration were always measured to ensure that there were no complications arising from the interference with the relevant CT band.

Alternatively, the EDA complex was prepared in situ by mixing appropriate amounts of the electron acceptor and electron donor. In Figure 2, the concentrations were (top to bottom) as follows: (a) 0.14 M AB with 0.020, 0.013, 0.0066 M TCNE; (b) 0.0026 M DBH with 0.35, 0.25, 0.17, 0.11, 0.066, 0.035 M TCNE; (c) 0.0030 M DBO with 0.16, 0.14, 0.11, 0.091, 0.057 M TCNE in acetonitrile.

Since the X-ray crystallography indicated the EDA complex from DBO and TCNE to be formed with 2:1 stoichiometry, we examined the spectrophotometric behavior under two extreme conditions in which [DBO] ≫ [TCNE] and [TCNE] ≫ [DBO]. The results in Table IV indicate no substantial difference in the Benesi-Hildebrand behavior. We thus conclude that if the 1:1 complex is formed, it is substantially less stable than the 2:1 complex.

Charge-Transfer Photochemistry of Azoalkane Complexes. A saturated solution of the EDA complex was prepared by dissolving the crystals in 2 mL of acetonitrile to make an apparent 0.02 M solution. It was irradiated for 15–30 min with light from the 450-W Xenon lamp by using a Pyrex cutoff filter at λ < 380 nm (Corning no. CS 375). Either the CT absorbance was measured spectrophotometrically or the ¹H NMR spectrum of the photolyzed solution was recorded periodically to detect changes in the EDA complex.

When DBO was treated in this way with TCNE or silver nitrate, no change in either the CT spectrum or the ¹H NMR spectrum was detected. Since the crystalline complexes of DBO with iodine and perfluoroalkyl radical were not available, the complexes were prepared and irradiated in situ. No spectral changes were observed. On the other hand, when the DBO complexes with tetranitromethane were irradiated at λ > 425 nm, the light yellow solution darkened considerably within 10 min. The absorption spectrum of the irradiated solution indicated a shift from ~400 nm to beyond 500 nm. Similarly the irradiation of a solution of DBO and CBr₄ with λ > 380 nm caused a spectral shift from

(57) Liang, P. *Organic Syntheses*; Wiley: New York, 1955; Collect. Vol. III, p 803.

(58) All elemental analyses by Atlantic Microlab, Inc., Atlanta, GA.

Table V. Final Positional Parameters for Azoalkane Complexes^a

atom	x	y	z	B (Å ²)	atom	x	y	z	B (Å ²)
[(DBO) ₂ , TCNE]									
N1	0.6252 (3)	1.2405 (2)	0.1874 (2)	5.66 (5)	C9	0.9316 (4)	0.4543 (3)	0.2923 (3)	5.56 (6)
N2	0.8242 (3)	1.0077 (2)	0.6612 (2)	5.66 (5)	H4	0.6008	0.5026	0.3467	5*
N3	0.6906 (2)	0.6844 (2)	0.3899 (2)	4.00 (4)	H5A	0.5085	0.7726	0.1398	5*
N4	0.8197 (2)	0.7734 (2)	0.3371 (2)	4.10 (4)	H5B	0.6786	0.6259	0.0668	5*
C1	0.5778 (3)	1.0410 (2)	0.4736 (2)	3.22 (4)	H6A	0.7366	0.9316	0.0463	5*
C2	0.7167 (3)	1.0231 (2)	0.5769 (2)	3.78 (4)	H6B	0.9068	0.7848	-0.0266	5*
C3	0.6058 (3)	1.1522 (2)	0.3142 (2)	3.82 (4)	H7	1.0632	0.8269	0.1544	5*
C4	0.7053 (3)	0.5745 (2)	0.2987 (2)	4.63 (5)	H8A	1.1848	0.5311	0.3091	5*
C5	0.6594 (4)	0.6955 (3)	0.1355 (2)	6.14 (6)	H8B	1.1790	0.5440	0.1313	5*
C6	0.8173 (4)	0.8054 (3)	0.0708 (3)	6.34 (7)	H9A	0.9586	0.3714	0.3998	5*
C7	0.9611 (3)	0.7532 (2)	0.1933 (2)	4.67 (5)	H9B	0.9496	0.3871	0.2217	5*
C8	1.0892 (4)	0.5637 (3)	0.2291 (3)	5.58 (6)					
[DBO, CBr ₄]									
Br1	0.1854 (2)	0.1119 (3)	0.177	2.63 (3)	C4	0.421 (3)	0.371 (4)	0.493 (2)	8.4 (9)
Br2	0.000	-0.3296 (5)	0.1501 (4)	4.6 (1)	H2	0.2399	0.4488	0.3870	6*
Br3	0.000	0.0104 (9)	-0.0439 (3)	4.87 (9)	H3A	0.3680	0.7731	0.4364	6*
N	0.435 (2)	0.334 (3)	0.294 (2)	5.5 (5)	H3B	0.3681	0.7415	0.3013	6*
C1	0.000	-0.040 (4)	0.124 (3)	3.3 (8)	H4A	0.3834	0.2140	0.5034	6*
C2	0.357 (2)	0.464 (5)	0.388 (2)	5.8 (7)	H4B	0.3835	0.4596	0.5575	6*
C3	0.408 (3)	0.686 (4)	0.374 (2)	7.4 (9)					
[DBO, AgNO ₃]									
Ag	0.51695 (4)	0.4300 (1)	0.12948 (5)	4.73 (2)	C4'	0.1537 (4)	-0.200 (1)	0.4684 (6)	4.3 (2)
O1	0.4764 (3)	0.6923 (9)	0.2349 (5)	5.8 (2)	C5'	0.1871 (6)	-0.288 (2)	0.6592 (8)	7.4 (3)
O2	0.3955 (4)	0.6306 (9)	0.0952 (5)	6.5 (2)	C6'	0.2102 (5)	-0.182 (2)	0.5751 (8)	6.3 (3)
O3	0.3810 (3)	0.8357 (8)	0.2046 (5)	5.8 (2)	C7'	0.1172 (6)	-0.498 (1)	0.5203 (9)	7.2 (3)
N1	0.4163 (4)	0.7192 (9)	0.1769 (5)	4.3 (2)	C8'	0.1420 (5)	-0.395 (1)	0.4370 (8)	6.3 (3)
N2	0.5657 (4)	0.721 (1)	0.0019 (5)	4.1 (2)	H5A	0.5699	1.0587	0.0713	6*
N3	0.5872 (3)	0.6426 (9)	0.0892 (5)	3.8 (2)	H5B	0.6543	1.1012	0.0679	6*
C1	0.6100 (5)	0.866 (1)	-0.0163 (7)	5.7 (2)	H6A	0.6133	0.9175	0.2268	6*
C4	0.6555 (5)	0.705 (1)	0.1596 (7)	5.0 (2)	H6B	0.6977	0.9536	0.2211	6*
C5	0.6196 (6)	1.003 (1)	0.0746 (9)	6.9 (3)	H7A	0.6782	0.6878	-0.0709	6*
C6	0.6486 (6)	0.903 (1)	0.1793 (8)	7.2 (3)	H7B	0.7197	0.8802	-0.0132	6*
C7	0.6813 (6)	0.781 (2)	-0.0084 (8)	8.2 (3)	H8A	0.7576	0.7407	0.1387	6*
C8	0.7081 (5)	0.685 (2)	0.0956 (9)	7.7 (3)	H8B	0.7158	0.5486	0.0812	6*
Ag'	0.01423 (3)	0.0777 (1)	0.38365 (5)	4.40 (2)	H5A'	0.2216	-0.3939	0.6899	6*
O1'	0.0244 (8)	0.3198 (9)	0.2489 (5)	5.7 (2)	H5B'	0.1830	-0.2039	0.7213	6*
O2'	0.1143 (3)	0.1579 (9)	0.3099 (5)	6.0 (2)	H6A'	0.2588	-0.2332	0.5681	6*
O3'	0.1131 (4)	0.361 (1)	0.1943 (5)	7.6 (2)	H6B'	0.2177	-0.0450	0.5964	6*
N1'	0.0850 (4)	0.279 (1)	0.2501 (5)	4.4 (2)	H7A'	0.1511	-0.6069	0.5547	6*
N2'	0.0702 (3)	-0.2162 (9)	0.5588 (5)	3.9 (2)	H7B'	0.0654	-0.5533	0.4878	6*
N3'	0.0881 (3)	-0.1332 (9)	0.4872 (5)	3.7 (2)	H8A'	0.1039	-0.4076	0.3630	6*
C1'	0.1149 (5)	-0.367 (1)	0.6099 (7)	5.1 (2)	H8B'	0.1897	-0.4540	0.4327	6*

^a Anisotropically refined atoms are given in the form of the isotropic equivalent thermal parameter defined as $(4/3)[a^2B(1,1) + b^2B(2,2) + c^2B(3,3) + ab(\cos \gamma)B(1,2) + ac(\cos \beta)B(1,3) + bc(\cos \alpha)B(2,3)]$. Asterisk identifies atom refined isotropically.

400 nm to > 480 within 20 min. The CT irradiation of the EDA complex of DBO and mercury(II) acetate with $\lambda > 415$ nm afforded a solution showing a shoulder at ~500 nm with a long tail to beyond 550 nm.

Measurement of the Cation-Radicals from the γ -Radiolysis of Azoalkanes. Samples for irradiation were prepared by dissolving the azoalkane in trichlorofluoromethane to make $\sim 10^{-2}$ M solutions. Each solution was placed in a 5-mm suprasil quartz tube which was degassed by 3 successive freeze-pump-thaw cycles and then sealed in vacuo. The sample tubes were immersed in liquid nitrogen and placed in the chamber of the ⁶⁰Co source for periods of 30 min to an hour. The dose rate at the center of the chamber as measured by ferrous sulfate actinometry per specification QA3-2 of quality control was 1×10^6 rad h⁻¹. The samples tubes were placed in the cavity of the ESR spectrometer which was maintained at 100 K by a flow of cold nitrogen gas. The irradiations with the visible light were effected with a focussed beam of the 1-kW mercury-xenon lamp filtered at $\lambda > 410$ nm. The ESR spectra were examined repeatedly at several temperatures. The only example in which an irreversible spectral change was observed is in the transition from spectrum A to B in Figure 14. The ESR spectrum A shows no obvious signs of one or more nitrogen splittings suggestive of an azoalkane cation-radical or related entity. In order to evaluate the magnitude of the nitrogen splitting in such species, we carried out MNDO/UHF calculations⁵⁹ on a planar cis diimide cation-radical as a function of reasonable

HNN angles.⁵⁵ The results indicate nitrogen s spin densities of $\rho_s(N) = 0.0677, 0.0855, \text{ and } 0.960$ for HNN angles of 100, 110, and 120°. These correspond to nitrogen hyperfine splittings of $a_N = 26, 32, \text{ and } 36$ G, respectively, by employing a proportionality constant of 379.⁶⁰ Clearly these values of a_N are all too large to remain unresolved outside of the line widths in spectrum A. If so, the paramagnetic species responsible for spectrum A has already lost nitrogen. Replacement of both hydrogens in this model with alkyl groups is unlikely to cause major changes in these estimates of a_N .⁶¹

X-ray Crystallography of the EDA Complexes of Azoalkanes with Sacrificial and Inequivalent Electron Acceptors. [(DBO)₂, TCNE]. A large reddish orange prism having dimensions 0.60 × 0.40 × 0.40 mm was mounted on a glass fiber in a random orientation on an Enraf-Nonius CAD-4 automatic diffractometer. The radiation used was Mo K α monochromatized by a dense graphite crystal assumed for all purposes to be 50% imperfect. Final cell constants as well as other information pertinent to data collection and refinement are listed in Table II. The Laue symmetry was determined to be 1, and the space group was shown to be either P1 or P $\bar{1}$. The original sample sublimed within 8 h at room temperature. Consequently, a second crystal of the same size was coated with a thin film of epoxy resin prior to mounting. Intensities were

(60) Pople, J. A.; Beveridge, D. L.; Dobosh, P. A. *J. Am. Chem. Soc.* **1968**, *90*, 4021.

(61) Compare Adams, J. Q.; Thomas, J. R. *J. Chem. Phys.* **1963**, *39*, 1904 with Nelsen, S. F.; Weisman, G. R.; Hintz, P. J.; Olp, D.; Fahey, M. R. *J. Am. Chem. Soc.* **1974**, *96*, 2916.

(59) Dewar, M. J. S.; Thiel, W. *J. Am. Chem. Soc.* **1977**, *99*, 4889, 4907. Program No. 353, Quantum Chemistry Program, Indiana University, Bloomington, IN.

measured by using the θ - 2θ scan technique, with the scan rate depending on the net count obtained in rapid prescans of each reflection. Two standard reflections were monitored periodically during the course of the data collection as a check of crystal stability and electronic reliability. These did not vary significantly. In reducing the data, Lorentz and polarization factors were applied; however, no correction for absorption was made due to the small absorption coefficient. Originally, the structure was thought to be comprised of a 1:1 mixture of TCNE and DBO. However, the calculated density made no sense for such a ratio, but a 2:1 ratio was reasonable. Since only TCNE could lie ordered about an inversion center, the assumption was made that there were two DBO per TCNE. A subsequent elemental analysis and the measurement of the density provided confirmation. The structure was solved by MULTAN,⁶² which revealed the positions of all but three of the nonhydrogen atoms in the asymmetric unit, which comprises one full DBO and one-half TCNE in space group $P\bar{1}$. Refinement was quite difficult owing to the very small scale factor involved. Eventually the remaining non-hydrogen atoms were located. The usual sequence of isotropic and anisotropic refinement was followed, after which all hydrogens were entered in ideally calculated positions. Hydrogen isotropic temperature factors were estimated based on the thermal motion of the associated carbons. After all shift/esd ratios were less than 0.1, convergence was reached at the agreement factors listed in Table II. No unusually high correlations were noted between any of the variables in the last cycle of least-squares refinement, and the final difference density map showed no peaks greater than $0.1 \text{ e } \text{\AA}^{-3}$. All calculations were made by using Molecular Structure Corporation's TEXRAY 230 modifications of the SDP-PLUS series of programs. The final positional parameters of [(DBO)₂, TCNE] are included in Table V. In the crystal there are no nonbonded interactions, especially those related to carbon atoms C₄-C₉ (or hydrogen atoms H₄-H₉), which are shorter than the sum of the van der Waals radii. Thus the tilt of the DBO donor described in Figure 8 is unlikely to arise from intermolecular interactions or packing forces.

[DBO, AgNO₃]. A large canary yellow diamond-shaped plate of dimensions $0.50 \times 0.50 \times 0.15 \text{ mm}$ was mounted on an Enraf-Nonius CAD-4 automatic diffractometer and otherwise treated as described above. The Laue symmetry was determined to be $2/m$, and from the systematic absences noted the space group was shown unambiguously to be $P2_1/c$. Intensities were measured by using the θ - 2θ scan technique, with the scan rate depending on the net count obtained in rapid prescans of each reflection. Two standard reflections were monitored periodically during the course of the data collection as a check of crystal stability and electronic reliability. These showed a slow, anisotropic decay ($\sim 25\%$) over the course of the experiment. A linear decay correction was made to partially account for this decay. In reducing the data, Lorentz and polarization factors were applied; however, no correction for absorption was made. The structure was solved by MULTAN,⁶² which revealed the positions of two independent Ag atoms in the asymmetric unit. This was not altogether unexpected since the exact nature of the molecular complex was not known. The remaining non-hydrogen atoms were slowly discovered in subsequent difference Fourier syntheses and finally revealed the EDA complex to consist of a 1:1 mixture of AgNO₃ and azoalkane. The usual sequence of isotropic and anisotropic refinement was followed, after which all hydrogens were entered into ideally calculated positions. Hydrogen temperature factors were estimated based on the thermal motion of the associated carbons. After all shift/esd ratios were less than 0.1, convergence was reached at the agreement factors listed in Table II. No unusually high correlations were noted between any of the variables in the last cycle of least-squares refinement. The final difference density map showed no peaks greater than $0.80 \text{ e } \text{\AA}^{-3}$. As can be seen in the packing diagram in Figure 10, the complex consists of two-dimensional,

polymeric layers consisting of an inner network of AgNO₃ insulated by DBO, as shown in Figure 13. All calculations were made by using Molecular Structure Corporation's TEXRAY 230 modifications of the SDP-PLUS series of programs. The final positional parameters of [DBO, AgNO₃] are included in Table V.

[DBO, CBr₄]. A large, irregular, clear, almost colorless crystal of dimensions $0.60 \times 0.40 \times 0.30 \text{ mm}$ was mounted on the diffractometer, as described above. The Laue symmetry was determined to be mmm , and from the systematic absences noted the space group was shown to be either $Pmc2_1$, $Pma2$, or $Pmma$. Since both components in this EDA complex could conceivably occupy mm symmetry sites, space group $Pmma$ was initially assumed, and the data were collected with the crystallographic axes oriented as such. Intensities were measured by using the θ - 2θ scan technique, with the scan rate depending on the net count obtained in rapid prescans of each reflection. Two standard reflections were monitored periodically during the course of the data collection as a check of crystal stability and electronic reliability. These did not vary significantly. In reducing the data Lorentz and polarization factors were applied, as well as an empirical absorption correction based on the measurement of five reflections having χ values near 90° .⁶³ Analysis of the unitary structure factors showed acentric statistics, and thus space group $Pmma$ was temporarily ruled out. Examination of the Patterson map showed the expected $1/2, 0, 2Z$ Harker line for $P2_1ma$ (transformed $Pmc2_1$), but not $1/2, 2Y, 0$ and $1/2, 0, 0$ for $Pm2a$ (transformed Pma). Therefore space group $Pmc2_1$ was chosen to attempt an initial structure solution. The data and cell constants were converted to the conventional $Pmc2_1$ setting, and the structure was quickly revealed by use of MULTAN.⁶² This 1:1 EDA complex is found to consist of linear polymeric chains running parallel to a , with alternating CBr₄ and DBO molecules lying on different mirror planes. This arrangement resulted in $1/2$ of each type of molecule in the asymmetric unit. The usual sequence of isotropic and anisotropic refinement was followed, after which all hydrogens were entered in ideally calculated positions. Upon examination of the positioning of the molecules in the unit cell, it became clear that they would not be able to conform to mm or $2/m$ sites. Thus no attempt was made to refine the structure in the higher symmetry $Pmma$. In order to determine the sense of direction in this polar space group, the inverse coordinate set was refined. It yielded values of R and R_w of 0.056 and 0.046, respectively, and so the reported atomic coordinates are assumed to be more probably correct. After all shift/esd ratios were less than 0.1, convergence was reached at the agreement factors listed in Table II. No unusually high correlations were noted between any of the variables in the last cycle of least-squares refinement. The final difference density map showed only two peaks larger than $1.00 \text{ e } \text{\AA}^{-3}$, both situated near Br₁. All calculations were made by using Molecular Structure Corporation's TEXRAY 230 modifications of the SDP-PLUS series of programs. The final fractional coordinates of [DBO, CBr₄] are included in Table V.

Acknowledgment. We thank Dr. L. Kevan for the use of his ⁶⁰Co source, Dr. J. D. Korp for assistance with the X-ray crystal structures of the EDA complexes, and the National Science Foundation and the Robert A. Welch Foundation for financial support.

Supplementary Material Available: Lists of the structure factor amplitudes and calculated atomic coordinates for the non-hydrogen atoms in the EDA complexes of DBO with tetracyanoethylene, carbon tetrabromide, and silver(I) nitrate (22 pages). Ordering information is given on any current masthead page.

(62) Germain, G.; Main, P.; Woolfson, M. M. *Acta Crystallogr., Sect. A: Cryst. Phys., Diffr., Theor. Gen. Crystallogr.* **1971**, *A27*, 368.

(63) North, A. C. T.; Phillips, D. C.; Matthews, F. S. *Acta Crystallogr., Sect. A: Cryst. Phys., Diffr., Theor. Gen. Crystallogr.* **1968**, *A24*, 351.